

Alma Mater Studiorum Università di Bologna  
Archivio istituzionale della ricerca

Unusual Cross-Linked Polystyrene by Copper-Catalyzed ARGET ATRP Using a Bifunctional Initiator and No Cross-Linking Agent

This is the final peer-reviewed author's accepted manuscript (postprint) of the following publication:

*Published Version:*

Braidi N., Buffagni M., Buzzoni V., Ghelfi F., Parenti F., Focarete M.L., et al. (2021). Unusual Cross-Linked Polystyrene by Copper-Catalyzed ARGET ATRP Using a Bifunctional Initiator and No Cross-Linking Agent. *MACROMOLECULAR RESEARCH*, 29(4), 280-288 [10.1007/s13233-021-9039-y].

*Availability:*

This version is available at: <https://hdl.handle.net/11585/844419> since: 2022-01-09

*Published:*

DOI: <http://doi.org/10.1007/s13233-021-9039-y>

*Terms of use:*

Some rights reserved. The terms and conditions for the reuse of this version of the manuscript are specified in the publishing policy. For all terms of use and more information see the publisher's website.

This item was downloaded from IRIS Università di Bologna (<https://cris.unibo.it/>).  
When citing, please refer to the published version.

(Article begins on next page)

This is the final peer-reviewed accepted manuscript of:

**N. Braidì, M. Buffagni, V. Buzzoni, F. Ghelfi, F. Parenti, M. L. Focarete, C. Gualandi, E. Bedogni, L. Bonifaci, G. Cavalca, A. Ferrando, A. Longo, I. Morandini, N. Pettenuzzo. Unusual cross-linked polystyrene by copper-catalyzed ARGET ATRP using a bifunctional initiator and no cross-linking agent. Macromolecular Research, 2021, 29, 280-288**

The final published version is available online at:

**<https://doi.org/10.1007/s13233-021-9039-y>**

Terms of use:

Some rights reserved. The terms and conditions for the reuse of this version of the manuscript are specified in the publishing policy. For all terms of use and more information see the publisher's website.

*This item was downloaded from IRIS Università di Bologna (<https://cris.unibo.it/>)*

***When citing, please refer to the published version.***



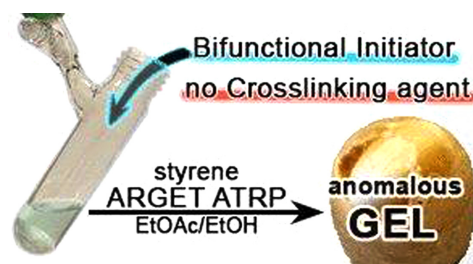
# Unusual Cross-Linked Polystyrene by Copper-Catalyzed ARGET ATRP Using a Bifunctional Initiator and No Cross-Linking Agent

1

2

3

**Abstract:** An anomalous polystyrene gel was obtained during the copper-catalyzed “activators regenerated by electron transfer” “atom transfer radical polymerization” (ARGET ATRP) of styrene at 60–70 °C, using ascorbic acid/ $\text{Na}_2\text{CO}_3$  as the reducing system and EtOAc/EtOH as the solvent mixture. The result is remarkable since no branching nor cross-linking reagents were added to the reaction mixture and their formation *in situ* was excluded. The anomalous PS branching, at the origin of the phenomenon, requires a generic bifunctional initiator and is mechanistically bound to termination reactions between bifunctional macroinitiators. As a matter of fact, the branching/cross-linking phenomenon loses intensity, or even disappears, under reaction conditions that cause the built-up of  $\text{Cu}^{\text{II}}$  or increase the chain polymerization rate. The temperature is also a critical variable since no branching was observed for temperatures higher than 90 °C. We believe that the route toward gelation starts with a controlled chain polymerization of styrene from the bifunctional initiator, soon integrated by a step-growth polymerization due to radical coupling of the terminal units. The progressive decrease in the number of chains and free radicals in the reaction mixture should make more and more probable the intramolecular coupling between the C–Cl ends of the remaining long and entangled chains, producing a polycatenane network.



The temperature is also a critical variable since no branching was observed for temperatures higher than 90 °C. We believe that the route toward gelation starts with a controlled chain polymerization of styrene from the bifunctional initiator, soon integrated by a step-growth polymerization due to radical coupling of the terminal units. The progressive decrease in the number of chains and free radicals in the reaction mixture should make more and more probable the intramolecular coupling between the C–Cl ends of the remaining long and entangled chains, producing a polycatenane network.

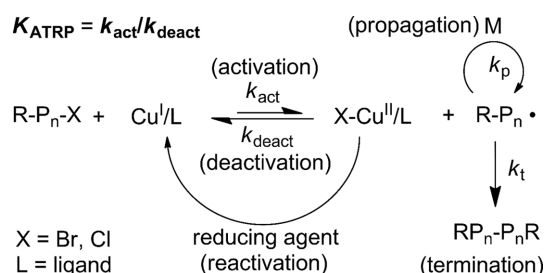
**Keywords:** styrene, cross-linked polystyrene, ARGET ATRP, copper, ascorbic acid, sodium carbonate, bifunctional initiators.

## 1. Introduction

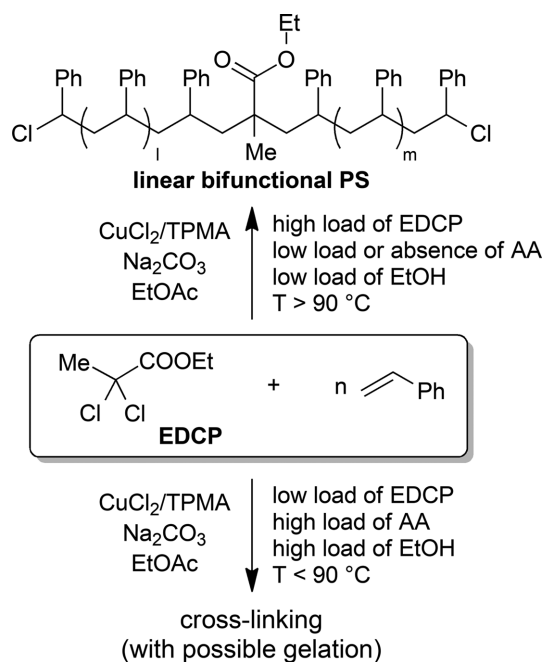
Among the reversible deactivation radical polymerization processes, atom transfer radical polymerization (ATRP) is likely the most popular and widespread.<sup>1–3</sup> The mechanism exploits a dynamic equilibrium between dormant species  $\text{R-P}_n\text{-X}$  and growing radicals  $\text{R-P}_n\cdot$  (Scheme 1). The equilibrium is promoted by a redox transition metal complex (typically copper with a polydentate nitrogen ligand).<sup>2–4</sup> The ATRP equilibrium aims to keep a low concentration of free radical species in the reaction mixture to avoid termination reactions and to allow the synthesis of controlled polymer chains with low dispersities ( $\bar{D}$ ).<sup>3</sup> The

atom transfers to and from the redox metal complex follow a concerted mechanism, *via* an inner-sphere electron transfer process.<sup>5</sup>

However, ATRP is not an ideal process because termination reactions cannot be completely suppressed. Consequently, the  $\text{X-Cu}^{\text{II}}/\text{L}$  species (deactivator) accumulates, bringing the polymer-



**Scheme 1.** Mechanism of a copper catalyzed ATRP process with reactivation of the redox complex.



**Scheme 2.** ARGET ATRP of styrene to synthesize controlled  $\alpha,\omega$  telechelic PS (*top*, previous works)<sup>23–25</sup> or gelation by topological cross linking *via* termination by radical coupling (*bottom*, this work).

ization to a stop. A relatively high amount of  $\text{Cu}^{\text{I}}/\text{L}$  (activator) is thus required to achieve satisfactory conversions. In order to work with a minimum level of metal and to by-pass the problem of its removal,<sup>6–8</sup> the catalytic system can be complemented by a “reducing agent” (Scheme 1), to regenerate the activator by reduction of the  $\text{X-Cu}^{\text{II}}/\text{L}$ .<sup>9</sup> The main regenerating methods are: i) “initiator for continuous activator regeneration” (ICAR) ATRP,<sup>10–12</sup> ii) “activators (re)generated by electron transfer” (A(R)GET) ATRP,<sup>13–16</sup> iii)  $\text{Cu}^0$ -promoted ATRP,<sup>17–19</sup> iv) electrochemical *e*ATRP,<sup>20</sup> and v) photo-ATRP.<sup>21,22</sup>

Recently, we reported about the ARGET ATRP in  $\text{EtOAc}/\text{EtOH}$  for the synthesis of polystyrene (PS) from a bifunctional initiator (ethyl 2,2-dichloropropionate, EDCP) (Scheme 2).<sup>23–25</sup> The process was catalyzed by  $\text{CuCl}_2/\text{tris}(2\text{-pyridylmethyl})\text{amine}$  (TPMA) and used ascorbic acid (AA)/ $\text{Na}_2\text{CO}_3$  as the reducing system. This ARGET ATRP system resulted from the successful adaptation of the ARGET atom transfer radical cyclization (ATRC) process we developed to efficiently synthesize  $\gamma$ -lactams from *N*-substituted *N*-allyl-2,2-dichloroamides.<sup>26</sup>

$\text{Na}_2\text{CO}_3$  has two crucial functions in the process. First, it removes the  $\text{HCl}$  released during the (re)generation of the catalyst. Second, it activates the reducing agent (AA) through deprotonation. No polymerization was indeed observed without  $\text{Na}_2\text{CO}_3$ .<sup>23</sup> Conversely, controlled polymerization was observed with  $\text{Na}_2\text{CO}_3$  alone (without AA).<sup>25</sup>

When the effect of the reaction temperature on our ARGET ATRP system was studied, an astonishing result was observed: the control abruptly deteriorated below  $90\text{ }^\circ\text{C}$  (Figure 1).<sup>23</sup> The surprising behavior can be better appreciated by looking at the dispersity and  $\Delta M_n\%$  (for the definition of  $\Delta M_n\%$  see the experimental section) of the isolated PSs *vs* temperature.

The loss of control was due to an unexpected branching,

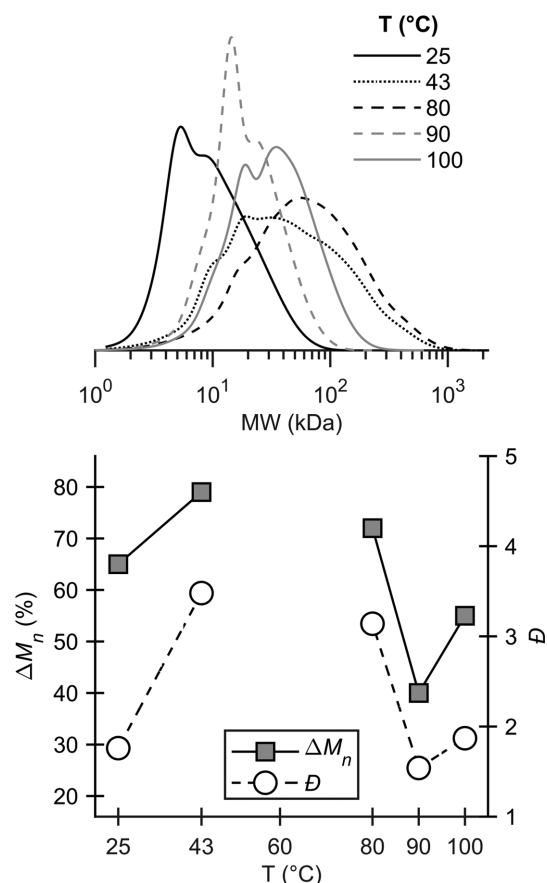
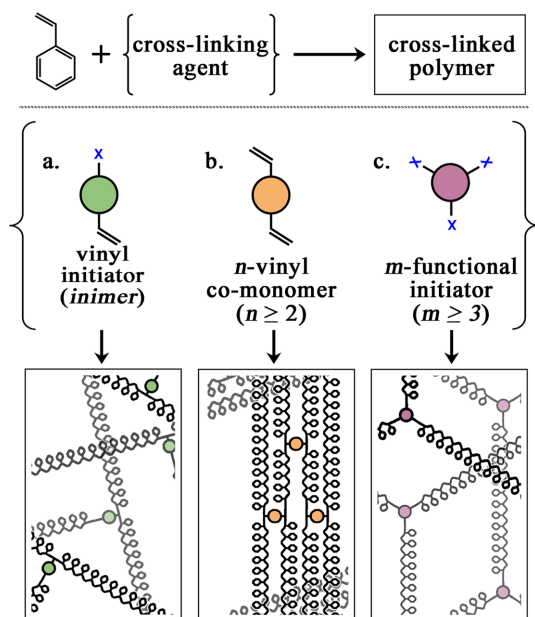


**Figure 1.** GPC analyses (*top*),  $\Delta M_n\%$  (■) and  $D$  (○) (*bottom*) of the PSs obtained at different temperature. Reaction conditions:  $[\text{S}]_0:[\text{EDCP}]_0:[\text{CuCl}_2]_0:[\text{TPMA}]_0:[\text{AA}]_0:[\text{Na}_2\text{CO}_3]_0 = 100:1.06:0.2:0.2:0.5:1.5$ ,  $V_{\text{EtOAc}} = 3\text{ mL}$ ,  $V_{\text{EtOH}} = 1\text{ mL}$ ,  $t = 18\text{ h}$ .

even if no cross-linking agents were added to the reaction mixture (Scheme 2). At  $60\text{ }^\circ\text{C}$ , the phenomenon was indeed so accentuated that the reaction mixture gelled, yielding a material insoluble in  $\text{CH}_2\text{Cl}_2$  and toluene,<sup>23</sup> two good solvents for PS.<sup>27</sup> The pyrolysis of this material excluded the presence of divinylbenzene and, accordingly, the *in situ* formation of any cross-linking agent. However, branching is thermosensitive, as highlighted by the recovered control when the reaction temperature was raised above  $90\text{ }^\circ\text{C}$  (Figure 1).

As far as we are aware, no one has ever reported this interesting cross-linking phenomenon during the ATRP of styrene. The synthesis of branched or cross-linked polymers by ATRP is however known and widely employed.<sup>28,29</sup> The strategies that can be utilized to achieve branching are three. The first strategy exploits the polymerization of inimers, alone or together with vinyl monomers (Scheme 3(a)).<sup>30,31</sup> The second one uses divinyl compounds as comonomers in an adequate amount<sup>32,33</sup> or homopolymerized *via* deactivation enhanced ATRP systems (Scheme 3(b)).<sup>34–36</sup> When no particular precaution is adopted, the use of divinyl compounds generally leads to the formation of insoluble networks.<sup>37,38</sup> The third and last strategy exploits instead the reaction between radical centers, *via* atom transfer radical coupling of multifunctional initiators (at least trifunctional) (Scheme 3(c)).<sup>39–41</sup>

In this paper, we report our initial studies about the unex-



**Scheme 3.** Three synthetic strategies to obtain branched PS networks, exploiting three different cross linking agents: (a) inimer, (b) multivinyl monomer, and (c) multifunctional initiator.

pected cross-linking observed in the ARGET ATRP of styrene in EtOAc/EtOH (3/1) at 60–70 °C with AA and Na<sub>2</sub>CO<sub>3</sub>. The experimental results rejected the *in situ* formation of cross-linking agents as the origin of the anomalous gelation. Since the use of a bifunctional initiator (EDCP) was required, we supposed that the unusual gelation may be rationalized as the generation of a polycatenane network.

## 2. Experimental

### 2.1. Materials

Styrene (S) (stabilized with 10–15 ppm of 4-*tert*-butylcatechol, TBC) was supplied by Versalis (Eni) S.p.A. (Italy). Absolute EtOH and EtOAc, the reaction solvents, were commercial products (>98%). MeOH and CH<sub>2</sub>Cl<sub>2</sub>, the solvents used for the reaction work-up, were commercial or recycled products. For the catalytic system, we used CuCl<sub>2</sub> “Riedel de Haën” (≥97%), TPMA “TCI Europe” (98%), AA “Sigma-Aldrich” (>99.5%), and Na<sub>2</sub>CO<sub>3</sub> “Carlo Erba” (≥99.5%). EDCP (GC purity ≥99%) was prepared by esterification of the 2,2-dichloropropionyl chloride (DCPC) with EtOH. DCPC was obtained following a literature method.<sup>42</sup> Methyl 2,2-dichlorobutanoate (MDCB) was obtained in an analogous way (GC purity >99%). Preparation of ethyl 2-chloroisobutyrate (ECiB) was achieved from ethyl 2-hydroxyisobutyrate adapting literature procedures.<sup>43,44</sup> Benzal chloride (BC), tin(II) 2-ethylhexanoate (Sn(EH)<sub>2</sub>), and ethyl methacrylate (EMA) were purchased from Merck and used without any purification. Well-controlled  $\alpha,\omega$ -dichloropolystyrenes were prepared using the “spurious” ARGET ATRP process we developed.<sup>25</sup>

### 2.2. Typical polymerization procedure (entry 13 of Table 1)

AA (0.130 mmol, 23.0 mg) and Na<sub>2</sub>CO<sub>3</sub> (0.391 mmol, 41.5 mg)

were weighed in a shuttle and transferred to an oven-dried 25 mL Schlenk tube.<sup>23</sup> After 3 cycles of vacuum/argon, the following reagents were added in the order: styrene (26.1 mmol, 3 mL), EtOAc (2 mL), EDCP (0.276 mmol, 47.2 mg) as solution in EtOAc (1 mL), EtOH (0.75 mL) and CuCl<sub>2</sub>/TPMA (0.0130 mmol, CuCl<sub>2</sub> 1.75 mg and TPMA 3.79 mg) as solution in EtOH (0.25 mL). The Schlenk tube was then immersed in an oil bath thermostated at 70 °C and the reaction mixture was stirred at 400 rpm (oval stirring bar:  $l=20$  mm,  $d=10$  mm) for 18 h. Afterward, the Schlenk tube was allowed to cool to room temperature. The gel was recovered (the operation was made easier adding 1–2 mL of MeOH), extracted in Soxhlet with MeOH (7 days), and dried in a vacuum oven till constant weight ( $T=60$  °C,  $P=1-2$  mmHg), yielding 2.25 g of cross-linked PS (83% yield).

When the final reaction mixture did not gel, it was diluted with CH<sub>2</sub>Cl<sub>2</sub>. The PS was then precipitated in MeOH (300 mL). To improve the coagulation, HClaq 10% w/v (2 mL) was added. The PS was isolated by filtration (filtering funnel with porosity P4), washed two times with MeOH, and kept under aspiration till constant weight (15–20 h). The conversion was estimated by subtracting the initiator contribution from the mass of the isolated material. Gravimetry is an easy and common method for conversion measurement. The error, due to the fractionation of PS chains with very low molecular weight during the reaction work-up, is however negligible for conversions that yield PS with  $M_n > 3000$  Da.<sup>45</sup> For the calculation of the  $M_n^{\text{th}}$ , the following equation was applied:  $M_n^{\text{th}} = \{[(\text{styrene moles}) / (\text{initiator moles})] \times M_{\text{styrene}} \times \text{conv} + M_{\text{initiator}}\}$ . The difference between  $M_n$  and  $M_n^{\text{th}}$  was expressed as  $\Delta M_n\%$ , i.e. the percentage difference between the experimental and the theoretical molar mass:  $\Delta M_n\% = [(M_n - M_n^{\text{th}}) / M_n] \times 100$ .

The quantity of a reagents is express as molar percentage (mol%) and it is always referred to the monomer.

Since MeOH is a good solvent for the redox complex, we preferred, for practical reasons, to avoid the typical filtration over basic Al<sub>2</sub>O<sub>3</sub> to remove the redox complex. The recovered PS was indeed white.

## 3. Results and discussion

### 3.1. Influence of the reagents ratios on the gelation process

Initial efforts to understand the causes of the atypical gelation examined the influence of reagent ratios (Table 1). The first tests aimed to decrease the amount of catalyst (0.2 mol%) to a more acceptable value (entries 1–3 of Table 1) and the reaction mixture gelled both using 0.1 or 0.05 mol% of CuCl<sub>2</sub>/TPMA (1/1). The lowest amount was considered adequate and was adopted as the standard for the following reactions.

The amount of EDCP was then halved from 1.06 mol% to 0.53 mol% (entry 4 of Table 1): no gelation occurred. However, the impressive  $\Delta M_n\%$  (85), the very large  $D$  (9.11), and the polymodality of the GPC chromatogram suggested that branching was indeed quite advanced (Figure 2).

The ratio  $[S]_0:[\text{EDCP}]_0 = [100]:[0.53]$ , used in the previous test, was otherwise obtained by doubling the volume of styrene (entry 5 of Table 1). In this case, the control over the polymerization seemed to be somewhat better, even if the GPC profile

**Table 1.** Effect of the reagents ratios on the gelation of styrene under ARGET ATRP conditions.<sup>a</sup>

Entry	EDCP (mol%)	CuCl <sub>2</sub> /TPMA (mol%)	AA/Na <sub>2</sub> CO <sub>3</sub> (mol%)	T/t (°C/h)	Conv. (%)	M <sub>n</sub> (kDa)	M <sub>n</sub> <sup>th</sup> (kDa)	ΔM <sub>n</sub> %	Đ
1	1.06	0.2	0.5/1.5	60/18	gel				
2	1.06	0.1	0.5/1.5	60/18	gel				
3	1.06	0.05	0.5/1.5	60/18	gel				
4	0.53	0.05	0.5/1.5	60/18	31	44.6	6.3	86	9.11
5 <sup>b</sup>	0.53	0.025	0.25/0.75	60/18	68	52.1	13.7	74	3.22
6	1.06	0.05	0.25/1.5	60/18	51	11.1	5.2	53	1.61
7	1.06	0.05	0.25/0.75	60/18	50	9.1	5.1	44	1.47
8	1.06	0.05	0.5/1.0	60/18	58	26.1	5.7	78	3.39
9	1.06	0.05	0.75/1.5	60/18	gel				
10 <sup>c</sup>	1.06	0.05	0.5/1.5	60/18	64	17.4	6.5	63	2.11
11 <sup>d</sup>	1.06	0.05	0.5/1.5	60/18	46	34.7	4.7	86	5.80
12	1.06	0.05	0.5/1.5	50/18	49	28.2	5.0	82	4.67
13	1.06	0.05	0.5/1.5	70/18	gel (79)				
14	1.06	0.05	0.5/1.5	60/4.5	41	17.5	4.2	76	2.79
15	1.06	0.05	0.5/1.5	70/4.5	52	25.8	5.3	79	3.69

<sup>a</sup>Conditions: V<sub>S</sub> = 3 mL, V<sub>EtOAc</sub> = 3 mL, V<sub>EtOH</sub> = 1 mL. <sup>b</sup>V<sub>S</sub> = 6 mL. <sup>c</sup>V<sub>EtOAc</sub> = 3.5 mL, V<sub>EtOH</sub> = 0.5 mL. <sup>d</sup>V<sub>EtOAc</sub> = 6 mL, V<sub>EtOH</sub> = 2 mL.

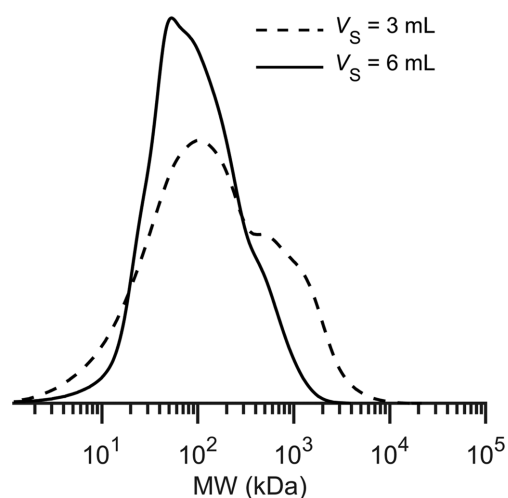


**Figure 2.** GPC analyses of the PSs synthesized with 3 mL (*dashed line*) and 6 mL (*solid line*) of styrene, with [S]<sub>0</sub>:[EDCP]<sub>0</sub> = [100]:[0.53] (entries 4 and 5 of Table 1).

resulted to be multimodal (Figure 2) and the ΔM<sub>n</sub>% and Đ appeared quite high. The multiangle laser light scattering (MALLS) analysis confirmed that this material was indeed branched (entry 3 of Table S1).

The lower polarity of the reaction mixture, after dilution with styrene, as previously observed in the ARGET ATRP at 100 °C with AA/Na<sub>2</sub>CO<sub>3</sub>,<sup>23</sup> makes the action of the reducing system milder, allowing a relatively higher concentration of Cu<sup>II</sup> in solution. This improves the control, even if quite partially.

Gelation was also greatly influenced by the amount of AA introduced. In fact, gelation did not occur either in its absence,<sup>25</sup> or lowering the load to 0.25 mol% (entry 6 of Table 1), or halving both AA and Na<sub>2</sub>CO<sub>3</sub> (entry 7 of Table 1; GPC trace Figure S8). Surprisingly, the PS isolated from the last two reactions (entries 6 and 7 of Table 1) showed some degree of control, even if not as good as without AA.<sup>25</sup> The “improvement” is likely due to a higher level of Cu<sup>II</sup> in the reaction mixture.

The [AA]<sub>0</sub>:[Na<sub>2</sub>CO<sub>3</sub>]<sub>0</sub> ratio was then increased from [1]:[3] to [1]:[2] by decreasing the amount of Na<sub>2</sub>CO<sub>3</sub> or by increasing the quantity of AA (entries 8 and 9 of Table 1, respectively). By decreasing Na<sub>2</sub>CO<sub>3</sub>, no gelation occurred but the recovered PS was likely branched due to the large ΔM<sub>n</sub>% (78) and Đ (3.39). By increasing AA instead, gelation was observed. However, the lower consistency of the isolated gel suggested that the material was less cross-linked than the one with a [AA]<sub>0</sub>:[Na<sub>2</sub>CO<sub>3</sub>]<sub>0</sub> ratio of [1]:[3] (entry 3 of Table 1).

Using a less polar environment (EtOAc/EtOH 3.5/0.5) the polymerization showed more control: ΔM<sub>n</sub>% = 63 and Đ = 2.11 (entry 10 of Table 1; Figure S9). Anyway, this result resembles the one recorded by doubling the volume of styrene (entry 5 of Table 1). Likely, the reasons for the slightly improved control are the same.

Also, the dilution of the reaction mixture prevented the gelation (entry 11 of Table 1): all the processes became understandably slower. However, the multimodality of the GPC curve (Figure S10) and the large ΔM<sub>n</sub>% (86) and Đ (5.80) tell us that the recovered polymer was probably branched.

All the previous observations agree with the mechanistic frame we traced for the ARGET ATRP process with AA/Na<sub>2</sub>CO<sub>3</sub> at 100 °C.<sup>23</sup> In short, reaction conditions, which allow a relatively higher concentration of Cu<sup>II</sup> in solution, yield a better control over the polymerization, hindering, as a consequence, the cross-linking phenomena.

Temperatures around 60 °C were then explored. No gelation occurred at 50 °C (entry 12 of Table 1). Probably, the branching process just became slower since the recovered material was clearly branched (as the high ΔM<sub>n</sub>% and Đ suggest). On the contrary at 70 °C, the reaction mixture gelled (entry 13 of Table 1), yielding a material more consistent and less sticky than the original one at 60 °C. The polymerizations at 60 and 70 °C (entries 3 and 13 of Table 1) were also filmed to record the gel point: 11–13 h at 60 °C and 7–9 h at 70 °C. Likely at 70 °C, the cross-linking process meets more favorable conditions. On the other hand, a further increase of the reaction temperature pro-

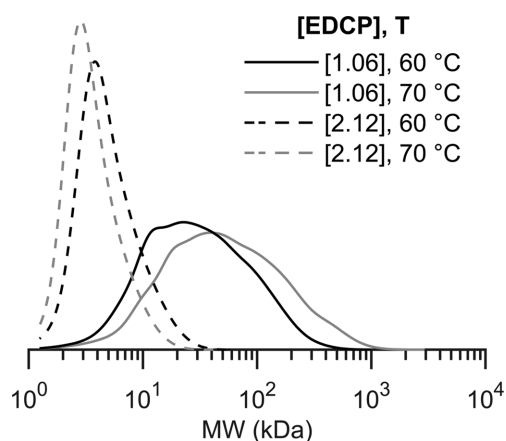


**Figure 3.** GPC of the PSs obtained after 4.5 h at 60 °C and 70 °C with 1.06 mol% (solid lines, entries 14 and 15 of Table 1) or 2.12 mol% (dashed lines, entries 1 and 2 of Table S2) of EDCP.

duced a decline of the phenomenon, rerouting polymerization toward a more typical controlled ATRP behavior (Figure 1).

The swelling degree of the gel obtained at 70 °C (entry 13 of Table 1) was also determined (Figure S1). The gel was found to be mildly cross-linked as the swelling degree (62.3) and the gel content (61%) suggest. A SEM image of the gel obtained at 70 °C (entry 13 of Table 1), after drying, is reported in Figure S2. It shows that the material is composed of cavities of different dimensions. Interestingly, in some of these cavities, single cubes of NaCl can be found (Figure S3). NaCl is the by-product of  $\text{CuCl}_2/\text{TPMA}$  (re)activation (Scheme S1).

Supposing that the events at the origin of branching may operate just at the early stages of the polymerization, the reaction time was shortened to 4.5 h (entries 14 and 15 of Table 1). The large  $\Delta M_n\%$ , the high  $\mathcal{D}$ , and the polymodal GPC (Figure 3) seem to confirm this supposition.

Finally, aiming to a more cross-linked material, the  $[\text{S}]_0:[\text{EDCP}]_0$  ratio was decreased to 100:2.12 by doubling the concentration of EDCP (entries 1-3 of Table S2). Surprisingly, no gelation occurred. Moreover, the recovered materials showed low dispersities ( $\mathcal{D} < 1.5$ ). These findings may be attributed to an increase of the  $\text{Cu}^{\text{II}}$  concentration in the reaction mixture, as the effect of the higher concentration of EDCP on the ATRP equilibrium (Scheme 1). In fact, gelation was recovered when the loads of AA and  $\text{Na}_2\text{CO}_3$  were also doubled (entry 4 of Table S2): a more reducing environment decreases the concentration of  $\text{Cu}^{\text{II}}$ , impairing the control over polymerization.

### 3.2. Polymerization kinetics

To have a better mechanistic frame of the gelation process, the kinetic analysis of the reaction at 70 °C was carried out (Table S3 and Figure 4). To prevent the gelation of the reaction mixture, the time-window was stopped at 6.5 h. The logarithmic curve (Figure 4, top) is linear until about 2 h, meaning that the radical concentration  $[\text{R}^{\cdot}]$  up until that point is approximately constant. Afterward, the radical concentration declines and, with it, the reaction rate too ( $\propto k_p \times [\text{R}^{\cdot}]$ ), owing to the annihilation of the C-Cl functions by radical termination. On the contrary,

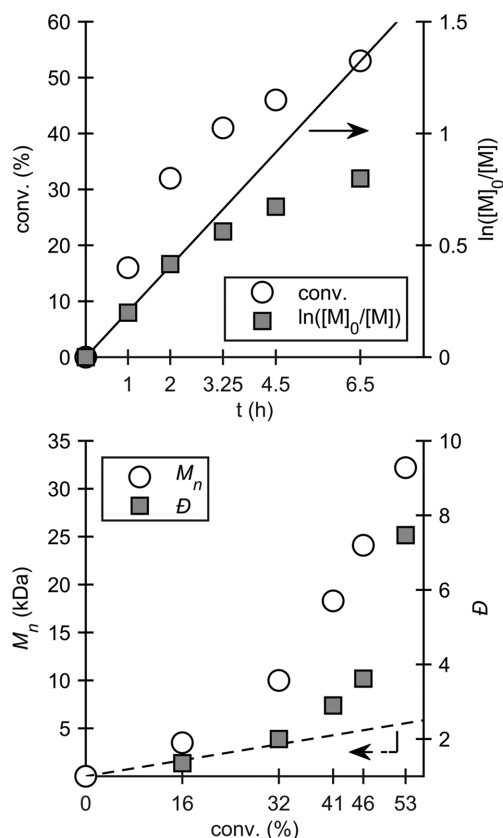


**Figure 4.** Results of the kinetic analysis. *Top:* conversion (○) and  $\ln([M]_0/[M])$  (■) vs time (the solid line shows the initial trend of the  $\ln([M]_0/[M])$ ). *Bottom:*  $M_n$  (○) and  $\mathcal{D}$  (■) vs conversion (the dashed line shows the trend of the  $M_n^{\text{th}}$ ). Conditions:  $[\text{S}]_0:[\text{EDCP}]_0:[\text{CuCl}_2]_0:[\text{TPMA}]_0:[\text{AA}]_0:[\text{Na}_2\text{CO}_3]_0 = 100:1.06:0.05:0.05:0.5:1.5$ ,  $V_{\text{S}} = 3$  mL,  $V_{\text{EtOAc}} = 3$  mL,  $V_{\text{EtOH}} = 1$  mL,  $T = 70$  °C.

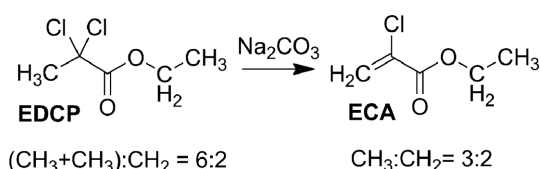
dispersity and  $M_n$  (Figure 4, bottom) increase progressively with the conversion. Considering that 6.5 h is close to the gel point, it is clear that the polymerization is out of control, as also highlighted by the GPC traces of the isolated PSs (Figure S4). The MALLS analysis of the PS recovered at 3.25 h showed that branching was already effective at that time (entry 3 of Table S3).

To note that the remarkable increase of  $M_n$ , after the first 2 h, is not related to the monomer conversion and is associated with a drop of the polymerization rate (a consequence of the decline of the C-Cl functions). This suggests that gel originates through the coupling of macrostructures. The annihilation of the halogenated functions was also supported by the NMR spectra of the PSs isolated after 1 h and 6.5 h, from which it can be appreciated the sharp drop of the area relative to the signals of the living chain ends (Figure S5 and Figure S6).

### 3.3. Mechanism of gelation

Since a base was present in the reaction mixture, gelation was initially attributed to the formation of ethyl 2-chloroacrylate (ECA) by partial dehydrohalogenation of EDCP (Scheme 4). In fact, ECA, being an inimer, can act both as monomer and initiator, thus inserting branching points in the polymer structure.<sup>46</sup>

However, we were unable to detect ECA from GC-MS analysis, even in the reaction mixtures lacking monomer and complex.



**Scheme 4.** Dehydrohalogenation of the initiator EDCP to the inimer ECA.

To support this hypothesis, we then tried the well-controlled ARGET ATRP of styrene without AA<sup>25</sup> in presence of variable amounts of methyl 2-chloroacrylate (MCA), a commercial analogous of ECA. Nonetheless, the control was not afflicted by the addition of MCA (25 and 50% compared to EDCP) (Table S4).

The formation of the ECA inimer was also disproved by <sup>1</sup>H-NMR signal integration. In fact, the dehydrohalogenation of EDCP to inimer ECA should change the CH<sub>3</sub>:CH<sub>2</sub> ratio from 6:2 to 3:2 (Scheme 4). For the <sup>1</sup>H-NMR analysis, deuterated PS was prepared adopting the same conditions of entry 13 of Table 1 but stopped after 1 h (Scheme S2), when all the initiator should have been completely consumed. The usage of styrene-d<sub>8</sub> leads to an easier discrimination between the broad aliphatic protons signals of the initiator (that resonate in the ranges 0.0–1.2 ppm and 2.4–3.8 ppm for CH<sub>3</sub> and CH<sub>2</sub>, respectively) and those of the polymer backbone chain (1.2–1.8 ppm). As a matter of fact, the <sup>1</sup>H-NMR spectrum of the deuterated PS (Figure S7) clearly shows that the ratio between the CH<sub>3</sub> and CH<sub>2</sub> signals of the initiator segments embedded in the polymeric chains is 6:2, getting rid of the inimer hypothesis definitively.

The radical transfer to polymer, involving the tertiary benzylic hydrogen of PS, was then considered as a possible cause of branching. To validate this hypothesis, the polymerization of styrene-d<sub>8</sub> was carried out under the conditions of entry 3 of Table 1. The reduced ease of cleavage of the C–D bond than the C–H bond (primary kinetic isotope effect) should prevent the inter-chain formation of benzylic radicals. Nonetheless, gelation was observed even with styrene-d<sub>8</sub>. Evidently, branching cannot be ascribed to the radical transfer to polymer. This result

also rules out the intervention of intra-chain migrations of the apical radical center and relative β-scission<sup>47,48</sup> as the cause of gelation, confirming that styrene has difficulty to branch in the absence of cross-linking agents.<sup>49</sup>

To understand if the type of reducing agent played a role, entries 13 and 15 of Table 1 were repeated, replacing AA with an equivalent amount of tin(II) 2-ethylhexanoate (Sn(EH)<sub>2</sub>) (entries 3–6 of Table 2). Sn(EH)<sub>2</sub> is a reducing agent widely employed in A(R)GET ATRP systems.<sup>14,50,51</sup> Surprisingly, cross-linking failed. Moreover, the isolated PS appeared linear (entry 5 of Table S1) and much more controlled than the one with AA (entries 4 and 6 of Table 2; the respective monomodal GPCs are reported in Figure S11). It would seem that the role of AA is more complex than that of a simply reducing agent. To remark that even with Sn(EH)<sub>2</sub>, no polymerization was observed in absence of Na<sub>2</sub>CO<sub>3</sub> (entries 1 and 2 of Table 2).<sup>23–25</sup>

Since styrene stabilized with 4-*tert*-butylcatechol (TBC) was used in all the previous tests, an experiment was carried out without the stabilizer (entry 7 of Table 2). The gelation of the reaction mixture excluded the involvement of TBC in the branching process.

To understand if bifunctionality of the initiator is a necessary condition, two polymerizations were carried out with ethyl 2-chloroisobutyrate (ECiB), the monofunctional initiator isosteric of EDCP (entries 8 and 9 of Table 2). In the first reaction, 1.04 mol% of ECiB were used (isomolar with EDCP), in the second reaction 2.08 mol% (same equivalents of halogenated functions of EDCP). In both cases, gelation was not observed. Even if the recovered PSs were not controlled, their relatively low dispersities ( $\bar{D} \sim 2.3$ ) and the monomodal GPC profiles (Figure S12) are quite different from the ones observed for the PS prepared from EDCP under the same conditions. The MALLS analysis confirmed that the PS from ECiB was indeed not branched (entry 6 of Table S1). These two last experiments teach us two things. First, the branching cannot originate from the formation of a cross-linking agent by side-reactions between styrene, copper complexes, AA, and Na<sub>2</sub>CO<sub>3</sub>. Second, bifunctionality is an

**Table 2.** Initiator and reducing agent effect on the gelation process.<sup>a</sup>

Entry	Initiator (mol%)	RA <sup>b</sup> (mol%)	Na <sub>2</sub> CO <sub>3</sub> (mol%)	T/t (°C/h)	Conv. (%)	M <sub>n</sub> (kDa)	M <sub>n</sub> <sup>th</sup> (kDa)	ΔM <sub>n</sub> %	$\bar{D}$
1	EDCP (1.06)	AA	0	70/4.5	0				
2	EDCP (1.06)	Sn(EH) <sub>2</sub>	0	70/4.5	0				
3	EDCP (1.06)	AA	1.5	70/4.5	52	25.8	5.3	79	3.69
4	EDCP (1.06)	Sn(EH) <sub>2</sub>	1.5	70/4.5	30	5.2	3.1	40	1.65
5	EDCP (1.06)	AA	1.5	70/18	gel (79%)				
6	EDCP (1.06)	Sn(EH) <sub>2</sub>	1.5	70/18	64	12.6	6.4	49	2.32
7 <sup>c</sup>	EDCP (1.06)	AA	1.5	70/18	gel				
8	ECiB (1.04)	AA	1.5	70/18	33	7.9	3.5	56	2.25
9	ECiB (2.08)	AA	1.5	70/18	63	7.9	3.3	58	2.38
10 <sup>d</sup>	MDCB (1.09)	AA	1.5	60/18	58	36.9	5.7	85	5.64
11	BC (1.04)	AA	1.5	60/18	gel				
12 <sup>e</sup>	MIPS (1.11)	AA	1.5	70/18	87	46.4	13.5	71	4.56
13 <sup>f</sup>	EDCP (1.06)	AA	1.5	60/18	95	20.4	10.4	49	1.52

<sup>a</sup>Conditions: [S]<sub>0</sub>:[RA]<sub>0</sub>:[CuCl<sub>2</sub>]<sub>0</sub>:[TPMA]<sub>0</sub> = 100:0.5:0.05:0.05, V<sub>S</sub> = 3 mL, V<sub>EtOAc</sub> = 3 mL, V<sub>EtOH</sub> = 1 mL. <sup>b</sup>Reducing Agent. <sup>c</sup>Non stabilized styrene was used. <sup>d</sup>Conditions: [S]<sub>0</sub>:[RA]<sub>0</sub>:[CuCl<sub>2</sub>]<sub>0</sub>:[TPMA]<sub>0</sub> = 100:0.5:0.2:0.2, EtOAc and EtOH were substituted by the same volumes of MeOAc and MeOH, respectively. <sup>e</sup>PS macroinitiator (MI<sub>PS</sub>): M<sub>n</sub> = 5.3 kDa,  $\bar{D}$  = 1.34. MI<sub>PS</sub> synthesis conditions: [S]<sub>0</sub>:[EDCP]<sub>0</sub>: [CuCl<sub>2</sub>]<sub>0</sub>: [TPMA]<sub>0</sub>: [AA]<sub>0</sub>: [Na<sub>2</sub>CO<sub>3</sub>]<sub>0</sub> = 100:0.53:0.025:0.025:0.25:0.75, V<sub>S</sub> = 6 mL, V<sub>EtOAc</sub> = 3.5 mL, V<sub>EtOH</sub> = 0.5 mL, T = 100 °C, t = 2 h. <sup>f</sup>Conditions: [EMA]<sub>0</sub>: [RA]<sub>0</sub>: [CuCl<sub>2</sub>]<sub>0</sub>: [TPMA]<sub>0</sub> = 100:0.2:0.2:0.2.

essential feature for the emerging of the gelation phenomenon. In fact, a cross-linked polymer was also obtained when EDCP was replaced with methyl 2,2-dichlorobutanoate (MDCB), another bifunctional initiator (entry 10 of Table 2). Although the gelation of the reaction mixture did not occur, it appeared indeed very viscous. In fact, the recovered PS showed a large dispersity ( $D = 5.64$ ) and a multimodal GPC profile (Figure S13). The MALLS analysis confirmed that this PS was indeed branched (entry 7 of Table S1).

Unlike EDCP, the dehydrohalogenation product of MDCB (i.e., methyl 2-chlorocrotonate) cannot be considered an inimer, since the steric hindrance on the  $\beta$ -carbon precludes the radical addition to the  $\alpha,\beta$ -unsaturated moiety, further questioning the inimer route to branching.<sup>52</sup> A definitive answer to the unsuitability of this model came from the gelation of PS when benzal chloride (BC), a molecule that cannot give dehydrohalogenation, was used as initiator (entry 11 of Table 2).

Being all the previous bifunctional initiators of geminal type and questioning that this was not a crucial condition, a linear bifunctional PS as macroinitiator (MIPS) was tested (entry 12 of Table 2). The relative GPC is reported in Figure 5. With satisfaction, a branched PS was obtained even with  $MI_{PS}$ , as the MALLS analysis (entry 8 of Table S1) and the GPC profile (Figure 5) attest.

In literature, it was reported about the hyperbranching of bifunctional PSs (precisely  $\alpha,\omega$ -dibromopolystyrenes) in a monomer-free ATRP system.<sup>53</sup> This produced, through radical coupling, a step-growth process, yielding a material similar to a hyperbranched polymer. It was suggested that this product was due to the formation of macroinimers or double unsaturated chains in the reaction mixture (Scheme 5), by dehydrohalogenation of the bifunctional chains. Since the  $Cu^{II}$ -catalyzed elimination can be virtually excluded in ARGET ATRP systems,<sup>54,55</sup> it was suggested the intervention of the nitrogen ligand.<sup>53</sup>

In our conditions, we believe that the dehydrohalogenation of the bifunctional chains is unsatisfactory for several reasons. Since elimination is susceptible to the temperature,<sup>56</sup> it is expected that at higher  $T$  the branching phenomenon should be enhanced, but the opposite was observed (Figure 1). Dehydrohalogenation is also governed by the bond strength of the atoms removed.<sup>57</sup>

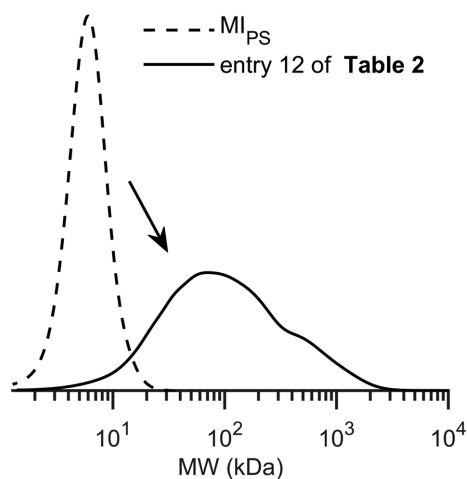
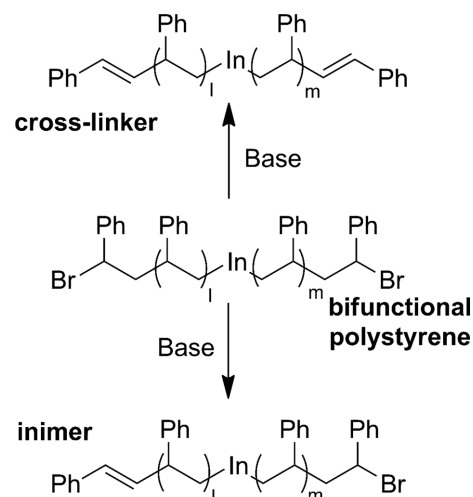


**Figure 5.** GPC analyses of the bifunctional macroinitiator  $MI_{PS}$  (dashed line) and of the PS obtained from  $MI_{PS}$  (solid line) (entry 12 of Table 2).



**Scheme 5.** Formation of unsaturated PS chain ends, responsible for branching in an ATRC coupling system using a bifunctional PS.<sup>53</sup>

Thus, it should be less effective when Cl (the atom we worked with) is used instead of Br and, even more, when the halide is removed as DCl, as in the case of deuterated PS. Not secondarily, the elimination would yield a  $\beta$ -substituted double bond that, owing to unfavorable steric interactions<sup>52</sup> with the incoming macroradical, cannot compete in the addition with the still present, more abundant and mobile monomer. In fact in our case, gelation occurred when nearly 50% of styrene was still present in the reaction mixture (Figure 4). Moreover, the  $^1H$ -NMR spectra of PSs from the kinetic study did not present the typical signals at 6.05 ppm and 6.15 ppm of the unsaturated chain ends (Figure S5).<sup>58</sup> Our considerations were also supported experimentally: no elimination was observed when a bifunctional PS25 was heated at 70 °C for 4.5 h in EtOAc/EtOH (without redox complex and replacing styrene with toluene), even in the presence of TPMA (see  $^1H$ -NMR, Figures S16-S18).

Summarizing, we can state that the anomalous PS branching is strictly related to the use of a generic bifunctional initiator and mechanistically related to the annihilation of the halogenated chain-end functions. Likely, the annihilation of the chain ends is the result of the termination by coupling between radicals. This converts a chain polymerization into a step-growth process because a bifunctional initiator (EDCP) is used.<sup>24,53,58</sup> The fact that termination reactions and gelation are interconnected is supported by the observation that the branching/cross-linking phenomenon loses intensity, or even disappears, under reaction conditions that slow down the reactivation of  $Cu^{II}$  (less polar environment or lower amount of AA and/or  $Na_2CO_3$ ), or push for its formation (higher initiator load) or, otherwise, increase the chain polymerization rate (higher monomer concentration).

Temperature is also a critical parameter for the occurrence of gelation. Indeed with temperatures above 90 °C, no branching was observed (Figure 1).<sup>23</sup> Besides, the relatively low reaction temperature prevents the termination between the macroradicals and the radicals generated by thermal autoinitiation of styrene.

Finally, the failed gelation with ethyl methacrylate (EMA)

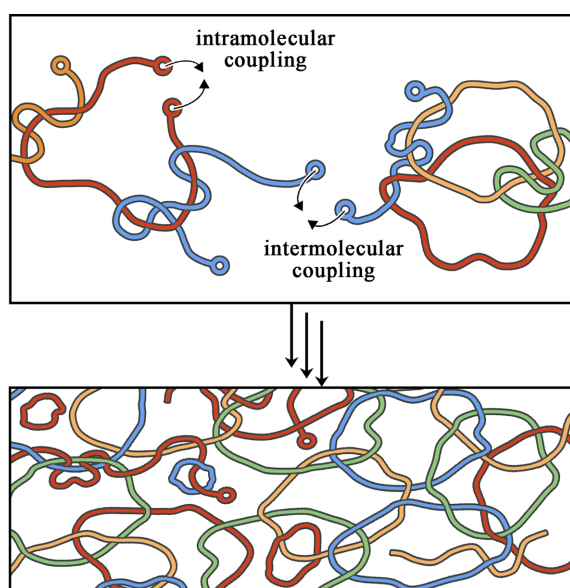
(entry 13 of Table 2), a monomer with a higher  $k_p/k_t$  than styrene and that preferentially terminates by disproportionation,<sup>59</sup> emphasizes how radical coupling is at the base of the phenomenon. The recovered polyethylmethacrylate (PEMA) is indeed not branched, as clearly suggested by the relatively narrow dispersity ( $D$  1.52). The bimodality of the GPC chromatogram (Figure S14) is probably a consequence of the disproportionation. In this way, two populations of PEMA are formed, one with two living ends and the other with only one.

Ascertained the importance of termination and radical coupling in the gelation process, the stoichiometry of the reduction process was examined. As reported in Scheme S1, the radical coupling requires 1 equivalent of AA (1 mol%) to be completed. This is two times the amount we were generally using. However, we had to take into account that  $\text{Cu}^{\text{II}}$  reactivation can be also performed by the combination of  $\text{Na}_2\text{CO}_3/\text{EtOH}$ ,<sup>25</sup> which is clearly *in surplus*.

To note that also the choice of the reducing agent seems to play a crucial role in branching, even if this point was not in-depth studied. In fact, in the absence of AA<sup>25</sup> or with  $\text{Sn}(\text{EH})_2$  (Table 2), the isolated PS resulted to be relatively controlled.

### 3.4. Hypotheses about the mechanisms

The reported experimental results suggest that the route toward gelation implies the formation of topological bonds. The polymerization starts with a controlled process from EDCP, which is soon integrated by a step-growth polymerization through termination by radical coupling. This implies a progressive decrease in the number of chains and free radicals in the reaction mixture. Consequently, the intramolecular coupling becomes more probable<sup>60</sup> between the C-Cl end functions of the remaining long and entangled chains.<sup>61</sup> The formation of macrocycles should depend also on the properties of the solvent. In a relatively poor solvent (like in our case), the polymer chains are led to a collapse, which increases the probability of ring closure.<sup>61</sup> In this way, a polycat-



**Scheme 6.** Formation of a polycatenane network, lacking real cross linking points.

enane network is formed and, as such, the resulting material is obviously lacking real cross-linking points (Scheme 6). It is quite likely that also the PS branching observed at 100 °C, when we used a load of EDCP < 1.06 mol%, has the same origin.<sup>23</sup>

Gelation starting from a bifunctional polymer is certainly an unusual phenomenon, but some examples are traceable in literature. Rigbi and Mark obtained an insoluble product while studying the chain extension of dihydroxy-terminated poly(dimethylsiloxane) with dimethyldiethoxysilane. The insoluble product was rationalized as a network of interlinked catenanes.<sup>62</sup> Recently, concatenated polysiloxane rings from heterotelechelic polysiloxane oligomers were prepared and actively studied.<sup>63,64</sup> A similar polycatenane network was also prepared by thermal polymerization of 1,2-dithiane.<sup>65</sup> Furthermore, a PS polycatenane network was synthesized by repeating the cycle between anionic polymerization with sodium naphthalenide and termination reaction with a dielectrophile in the same reaction flask, even if in very low yields.<sup>66</sup>

Finally, it must be recalled that various studies stressed that in the course of irreversible polycondensations, to which our system is strictly analogous, end-to-end cyclization competes with chain-growth at any stage and at any monomer concentration.<sup>67</sup>

## 4. Conclusion

This research tried to evaluate the critical variables of the atypical gelation of PS obtained at 60–70 °C in EtOAc/EtOH (3/1) during the  $\text{CuCl}_2/\text{TPMA}$  (1/1) catalyzed ARGET ATRP with AA/ $\text{Na}_2\text{CO}_3$  as the reducing system, and EDCP as bifunctional initiator. The formation of the cross-linked network is independent from the metal load (in the studied range) but, instead, it appears to be strongly influenced by the following factors: i) polarity of the medium, ii) volume of monomer, iii) mol% of AA, iv) mol% of  $\text{Na}_2\text{CO}_3$ , and v) monomer/initiator ratio. In brief, less polar environments, lower loads of AA/ $\text{Na}_2\text{CO}_3$ , or low monomer/initiator ratios allow for a milder activation of the redox complex, maintaining a sufficiently high concentration of  $\text{Cu}^{\text{II}}$  in the reaction mixture. As a consequence, the polymerization becomes more controlled and the cross-linking process slows down or, even, disappears.

Temperature and type of reducing agent are also critical parameters for the occurrence of gelation, since with temperatures above 90 °C or with  $\text{Sn}(\text{EH})_2$  in place of AA no branching was observed. At this time however, these aspects have not been well understood and require further studies.

The absence of the *in situ* formation of an inimer or a cross-linker species, the kinetic analysis, the need for monomers that terminates by coupling, and the necessity of a bifunctional initiator suggest that gelation may be the result of a progressive reductive coupling of the apical C-Cl functions of living PS chains, which should end with the creation of a polycatenane network. Further studies are in progress to substantiate this hypothesis, to clear the role of reaction temperature, AA, and catalyst, and to determine the physical properties of the material and their relationship with the reaction conditions. Additional results will be published in due course.

**Supporting information:** The supporting information report MALLS analyses, study on the increment of initiator concentration, kinetic study with relative  $^1\text{H}$ - and  $^{13}\text{C}$ -NMR spectra, polymerizations in presence of MCA, synthesis and NMR spectra of deuterated PS, selected GPC eluograms, and  $^1\text{H}$ -NMR spectra of the dehydrochlorination test on the  $\alpha,\omega$ -dichloropoly-styrene.

**Funding:** This study was funded by Versalis (Eni) S.p.A.

**Author Contributions:** All authors contributed to the study conception and design. Material preparation, data collection and analysis were performed by Niccolò Braidì, Mirko Buffagni, Franco Ghelfi, Francesca Parenti, Maria Letizia Focarete, Chiara Gualandi, Elena Bedogni, Luisa Bonifaci, Gianfranco Cavalca, Angelo Ferrando, Aldo Longo, Ida Morandini and Nicolò Petteuzzo. The first draft of the manuscript was written by Franco Ghelfi and all authors commented on previous versions of the manuscript. All authors read and approved the final manuscript.

## References

- (1) K. Matyjaszewski, *Adv. Mater.*, **30**, 1706441 (2018).
- (2) M. Ouchi, T. Terashima, and M. Sawamoto, *Chem. Rev.*, **109**, 4963 (2009).
- (3) P. Krysz and K. Matyjaszewski, *Eur. Polym. J.*, **89**, 482 (2017).
- (4) L. Fetzer, V. Toniazzo, D. Ruch, and F. di Lena, *Isr. J. Chem.*, **52**, 221 (2012).
- (5) C. Fang, M. Fantin, X. Pan, K. de Fiebre, M. L. Coote, K. Matyjaszewski, and P. Liu, *J. Am. Chem. Soc.*, **141**, 7486 (2019).
- (6) M. Ding, X. Jiang, L. Zhang, Z. Cheng, and X. Zhu, *Macromol. Rapid Commun.*, **36**, 1702 (2015).
- (7) Y. Shen, H. Tang, and S. Ding, *Prog. Polym. Sci.*, **29**, 1053 (2004).
- (8) E. A. Kandirmaz, E. N. Gençoğlu, and N. Kayaman Apohan, *Macromol. Res.*, **27**, 756 (2019).
- (9) N. V. Tsarevsky and K. Matyjaszewski, *Chem. Rev.*, **107**, 2270 (2007).
- (10) M. Lamson, M. Kopeć, H. Ding, M. Zhong, and K. Matyjaszewski, *J. Polym. Sci. Part A: Polym. Chem.*, **54**, 1961 (2016).
- (11) J. Sun, Y. Zhang, J. Li, Q. Ren, C. Wang, and Z. Xu, *J. Macromol. Sci. A*, **52**, 609 (2015).
- (12) C. Nishiura, V. Williams, and K. Matyjaszewski, *Macromol. Res.*, **25**, 504 (2017).
- (13) K. A. Payne, D. R. D'hooge, P. H. M. Van Steenberge, M. F. Reyniers, M. F. Cunningham, R. A. Hutchinson, and G. B. Marin, *Macromolecules*, **46**, 3828 (2013).
- (14) N. Chan, M. F. Cunningham, and R. A. Hutchinson, *Polym. Chem.*, **3**, 1322 (2012).
- (15) Y. Kwak and K. Matyjaszewski, *Polym. Int.*, **58**, 242 (2009).
- (16) C. Cheng, X. Bai, X. Zhang, M. Chen, Q. Huang, Z. Hu, and Y. Tu, *Macromol. Res.*, **22**, 1306 (2014).
- (17) D. Konkolewicz, Y. Wang, P. Krysz, M. Zhong, A. A. Isse, A. Gennaro, and K. Matyjaszewski, *Polym. Chem.*, **5**, 4396 (2014).
- (18) B. M. Rosen and V. Percec, *Chem. Rev.*, **109**, 5069 (2009).
- (19) A. Anastasaki, V. Nikolaou, G. Nurumbetov, P. Wilson, K. Kempe, J. F. Quinn, T. P. Davis, M. R. Whittaker, and D. M. Haddleton, *Chem. Rev.*, **116**, 835 (2016).
- (20) P. Chmielarz, M. Fantin, S. Park, A. A. Isse, A. Gennaro, A. J. D. Magenau, A. Sobkowiak, and K. Matyjaszewski, *Prog. Polym. Sci.*, **69**, 47 (2017).
- (21) S. Dadashi Silab, S. Doran, and Y. Yagci, *Chem. Rev.*, **116**, 10212 (2016).
- (22) X. Pan, M. A. Tasdelen, J. Laun, T. Junkers, Y. Yagci, and K. Matyjaszewski, *Prog. Polym. Sci.*, **62**, 73 (2016).
- (23) N. Braidì, M. Buffagni, F. Ghelfi, A. Menabue, M. Imperato, F. Parenti, A. Gennaro, A. A. Isse, E. Bedogni, L. Bonifaci, G. Cavalca, A. Ferrando, A. Longo, and I. Morandini, *Macromol. Res.*, **28**, 751 (2020).
- (24) F. Ghelfi, A. Longo, A. Ferrando, and M. Buffagni, WO 2019215626.
- (25) N. Braidì, M. Buffagni, F. Ghelfi, F. Parenti, A. Gennaro, A. A. Isse, E. Bedogni, L. Bonifaci, G. Cavalca, A. Ferrando, A. Longo, and I. Morandini, *J. Macromol. Sci. A*, (2021), DOI:10.1080/10601325.2020.1866434.
- (26) F. Bellesia, A. J. Clark, F. Felluga, A. Gennaro, A. A. Isse, F. Roncaglia, and F. Ghelfi, *Adv. Synth. Cat.*, **355**, 1649 (2013).
- (27) D. Braun, H. Cherdron, M. Rehahn, H. Ritter, and B. Voit, *Polymer Synthesis: Theory and Practice*, Springer, Berlin, 2013 (5th), p. 68, DOI:10.1007/978 3 642 28980 4.
- (28) X. Wang and H. Gao, *Polymers*, **9**, 188 (2017).
- (29) H. Gao and K. Matyjaszewski, *Prog. Polym. Sci.*, **34**, 317 (2009).
- (30) Z. C. Chen, C. L. Chiu, and C. F. Huang, *Polymers*, **6**, 2552 (2014).
- (31) X. Luo, S. Xie, W. Huang, B. Dai, Z. Lu, and D. Yan, *Chinese J. Polym. Sci.*, **34**, 77 (2016).
- (32) W. Huang, Y. Zheng, B. Jiang, D. Zhang, J. Chen, Y. Yang, C. Liu, G. Zhai, L. Kong, and F. Gong, *Macromol. Chem. Phys.*, **211**, 2211 (2010).
- (33) W. Huang, H. Yang, X. Xue, B. Jiang, J. Chen, Y. Yang, H. Pu, Y. Liu, D. Zhang, L. Kong, and G. Zhai, *Polym. Chem.*, **4**, 3204 (2013).
- (34) W. Wang, Y. Zheng, E. Roberts, C. J. Duxbury, L. Ding, D. J. Irvine, and S. M. Howdle, *Macromolecules*, **40**, 7184 (2007).
- (35) T. Zhao, Y. Zheng, J. Poly, and W. Wang, *Nat. Commun.*, **4**, 1873 (2013).
- (36) Q. Xu, S. A. P. McMichael, J. Creagh Flynn, D. Zhou, Y. Gao, X. Li, X. Wang, and W. Wang, *ACS Macro Lett.*, **7**, 509 (2018).
- (37) K. Kanamori, J. Hasegawa, K. Nakanishi, and T. Hanada, *Macromolecules*, **41**, 7186 (2008).
- (38) P. Polanowski, J. K. Jeszka, K. Krysiak, and K. Matyjaszewski, *Polymer*, **79**, 171 (2015).
- (39) A. Debuigne, M. Hurtgen, C. Detrembleur, C. Jérôme, C. Barner Kowollik, and T. Junkers, *Prog. Polym. Sci.*, **37**, 1004 (2012).
- (40) X. Jiang, Y. Chen, and F. Xi, *Macromolecules*, **43**, 7056 (2010).
- (41) C. Li and Q. Wang, *Polymer*, **99**, 594 (2016).
- (42) F. Bellesia, F. D'Anna, F. Felluga, V. Frenna, F. Ghelfi, A. F. Parsons, F. Reverberi, and D. Spinelli, *Synthesis*, **44**, 605 (2012).
- (43) N. Kanbayashi, K. Takenaka, T. Okamura and K. Onitsuka, *Angew. Chem. Int. Ed.*, **52**, 4897 (2013).
- (44) H. R. Hudson and G. R. de Spinoza, *J. Chem. Soc., Perkin Trans. I*, 104 (1976), DOI:10.1039/p19760000104.
- (45) M. Al Harthi, L. S. Cheng, J. B. P. Soares, and L. C. Simon, *J. Polym. Sci. Part A: Polym. Chem.*, **45**, 2212 (2007).
- (46) F. Li, M. Cao, Y. Feng, R. Liang, X. Fu, and M. Zhong, *J. Am. Chem. Soc.*, **141**, 794 (2019).
- (47) T. M. Kruse, O. S. Woo, H. W. Wong, S. S. Khan, and L. J. Broadbelt, *Macromolecules*, **35**, 7830 (2002).
- (48) P. H. M. Van Steenberge, J. Vandenberg, M. F. Reyniers, T. Junkers, D. R. D'hooge, and G. B. Marin, *Macromolecules*, **50**, 2625 (2017).
- (49) S. C. Thickett and R. G. Gilbert, *Macromolecules*, **38**, 9894 (2005).
- (50) L. Bai, L. Zhang, Z. Cheng, and X. Zhu, *Polym. Chem.*, **3**, 2685 (2012).
- (51) W. Jakubowski and K. Matyjaszewski, *Angew. Chemie Int. Ed.*, **45**, 4482 (2006).
- (52) H. Fischer and L. Radom, *Angew. Chemie Int. Ed.*, **40**, 1340 (2001).
- (53) T. Sarbu, K. Y. Lin, J. Ell, D. J. Siegwart, J. Spanswick, and K. Matyjaszewski, *Macromolecules*, **37**, 3120 (2004).
- (54) K. Matyjaszewski, K. Davis, T. E. Patten, and M. Wei, *Tetrahedron*, **53**, 15321 (1997).
- (55) W. Jakubowski, B. Kirci Denizli, R. R. Gil, and K. Matyjaszewski, *Macromolecules*, **35**, 7830 (2002).

- romol. Chem. Phys.*, **209**, 32 (2008).
- (56) M. B. Smith, *March's Advanced Organic Chemistry*, John Wiley & Sons, Hoboken (New Jersey), 2013 (7th), p. 1278.
- (57) M. B. Smith, *March's Advanced Organic Chemistry*, John Wiley & Sons, Hoboken (New Jersey), 2013 (7th), p. 1297.
- (58) C. Yoshikawa, A. Goto, and T. Fukuda, *e Polymers*, **2**, 013 (2002).
- (59) Y. Nakamura, T. Ogihara, and S. Yamago, *ACS Macro Lett.*, **5**, 248 (2016).
- (60) A. F. Voter and E. S. Tillman, *Macromolecules*, **43**, 10304 (2010).
- (61) Z. Jia and M. J. Monteiro, *J. Polym. Sci. Part A: Polym. Chem.*, **50**, 2085 (2012).
- (62) Z. Rigbi and J. E. Mark, *J. Polym. Sci. Part B: Polym. Phys.*, **24**, 443 (1986).
- (63) J. Goff, S. Sulaiman, B. Arkles, and J. P. Lewicki, *Adv. Mater.*, **28**, 2393 (2016).
- (64) P. Hu, J. Madsen, Q. Huang, and A. L. Skov, *ACS Macro Lett.* **9**, 1458 (2020).
- (65) K. Endo, T. Shiroi, and N. Murata, *Polym. J.*, **37**, 512 (2005).
- (66) B. Vollmert and J. X. Huang, *Makromol. Chem., Rapid Commun.* **2**, 467 (1981).
- (67) H. R. Kricheldorf, S. M. Weidner, and F. Scheliga, *Polym. Chem.*, **11**, 2595 (2020).

**Publisher's Note** Springer Nature remains neutral with regard to jurisdictional claims in published maps and institutional affiliations.

## Supporting Information

## 1. Preparation of the stock solutions and characterizations details

1.1. Preparation of the CuCl<sub>2</sub>/tris(2-pyridylmethyl)amine (TPMA) solution

CuCl<sub>2</sub> (351 mg, 2.61 mmol) was dissolved with absolute EtOH in a 10 mL volumetric flask. In a second 10 mL volumetric flask, a solution of TPMA (151.6 mg, 0.522 mmol) in 5 mL of absolute EtOH was prepared. To the TPMA solution, 2 mL of the first CuCl<sub>2</sub> solution were added and then EtOH was added to make up to the mark. The mixture was finally shaken till the complete dissolution of the complex.

## 1.2. Preparation of ethyl 2,2-dichloropropanoate (EDCP) solution

In a 10 mL volumetric flask, EDCP (400  $\mu$ L, 2.76 mmol) was added using a 500  $\mu$ L microsyringe. EtOAc is then added to make up to the mark.

## 1.3. Characterization

The molecular weight distributions, dispersity ( $D$ ), and molar mass averages ( $M_n$ ,  $M_w$ ,  $M_z$ ) of all the samples were obtained using a conventional GPC, equipped with only a concentration detector and calibrated with standards of monodisperse polymers matching those subsequently analyzed. In order to study the branching of some samples, a GPC-VISCO-MALLS equipped with a multiangle laser light scattering (MALLS) detector and a viscometer (VISCO) detector was used.

In conventional GPC, the molecular weight distributions were determined using a Waters GPC system composed of a Waters Alliance 2695 separation module and a Waters 2414 Differential Refractometer Detector. Empower 2 (Waters) was used as chromatographic analysis software. The system was calibrated with 20 narrow distribution standards of polystyrene (PS) with molecular weights ranging from 1300 Da to 7 000 000 Da. Four GPC Phenogel (Phenomenex) columns (size: 300  $\times$  7.6 mm, particle size: 5  $\mu$ m, porosity 10<sup>6</sup>, 10<sup>5</sup>, 10<sup>4</sup> and 10<sup>3</sup> Å) were connected

and housed in an oven at 30 °C. Tetrahydrofuran for HPLC was used as a mobile phase and the elution conditions were: flow rate 1 mL/min, injection volume 200  $\mu$ L, sample concentration 2.5 mg/mL, and toluene as internal standard.

GPC-VISCO-MALLS analyses were performed using the same GPC system additionally equipped with a MALLS DAWN EOS WYATT and Viscotek T50 A as light scattering and viscometer detectors. The analytical conditions were the same used in conventional GPC but the sample concentration was 1.0 mg/mL. Two different samples of broad distribution PS were used for comparison: a linear one (commercial product) and a branched one (synthesized from styrene and divinylbenzene).

<sup>1</sup>H-NMR spectra were recorded with a Bruker AV-400 spectrometer (resonance frequency 400.13 MHz) equipped with a 5 mm PABBO BB/19F-1H/D  $x, y, z$ -field gradient probe-head, with Topspin 3.6 software package, operating in Fourier transform. Typical acquisition parameters (<sup>1</sup>H, 400.13 MHz): 512 transients, spectral width 7.5 kHz, and a delay time of 7.0 s. Chemical shifts were referred to solvent peak. All the spectra were acquired using CDCl<sub>3</sub> as solvent at 298 K.

Images of the cross-linked PS were obtained with a SEM FEG TESCAN MIRA II (TESCAN). The sample was prepared by cutting a small amount of material that was then sputtered with Au (thickness  $\approx$  20 nm).

## 2. Multiangle laser light scattering analyses

The percentage difference ( $\Delta M_w\%$ ) was used as a rough parameter to evaluate the grade of branching.  $\Delta M_w\%$  is calculated as the relative difference between the real (or absolute) molecular weight determined by MALLS detector ( $M_{w-MALLS}$ ) and the molecular weight determined by conventional GPC ( $M_{w-GPC}$ ). The applied formula is  $\Delta M_w\% = (M_{w-MALLS} - M_{w-GPC}) / M_{w-MALLS}$ .

For each sequence of samples analyzed by GPC, two different samples of broad distribution PS were injected for comparison: a linear one and a branched one. A comparison with the resulting  $\Delta$  obtained on the branched polymer allowed us to clarify which synthesized materials are branched. Variations of the percentage difference higher than the 60% of the value recorded for the branched reference were taken as empirical

**Table S1.** MALLS analysis of selected PSs

Entry	PS (entry and Table)	$M_{w-MALLS}$ (kDa)	$M_{w-GPC}$ (kDa)	$M_{w-MALLS} / M_{w-GPC}$	$\Delta M_w\%a$
1	commercial linear	288.9	288.0	1.00	0.3
2	branched	387.2	316.8	1.22	18.2
3	#5 of Table 1	244.9	174.2	1.41	28.9
4	#3 of Table S3	60.3	47.5	1.27	21.2
5	#6 of Table 2	31.5	29.1	1.08	7.6
6	#9 of Table 2	19.5	18.9	1.03	3.1
7	#10 of Table 2	384.7	198.9	1.93	48.3
8	#12 of Table 2	377.2	228.5	1.65	39.4

<sup>a</sup>The PS is considered branched for  $\Delta M_w\% > 10.9\%$ .

boundary between a branched and a linear PS.

Table S1 summarizes the GPC-MALLS analysis. The  $\Delta M_w$  % of the branched standard was 18.2%, therefore the empirical boundary limit between linear and branched PS resulted to be 10.9% (i.e., the 60% of 18.2%).

### 3. Swelling, SEM images, and XR spectrum of the gel

The cross-linked product was removed from the Schlenk tube and cut lengthwise into three pieces, resulting in three discs. The central disc (~ 1 g) was then placed in a bottle with 50 mL of toluene, which is enough to completely cover the swollen disc. Every week, the supernatant was decanted off and replaced with new toluene. After three weeks of swelling, the disc was removed

from the bottle and carefully dried to deswell it (at first under a laboratory hood and then in a vacuum oven).

The swelling degree ( $Q$ ) and the gel content (% $G$ ) were calculated using the following equations.  $\rho_{PS}$  and  $\rho_{tol}$  are the densities of PS (1.05 g/mL) and toluene (0.867 g/mL), respectively.  $m_{dry}$  is the initial mass of PS before swelling, containing both the gel and the sol fraction.  $m_{wet}$  is the mass of the swollen PS gel in toluene.  $m_{res}$  is the mass of the residual cross-linked PS after deswelling (i.e., gel fraction).

$$Q = 1 + \left[ \frac{\rho_{PS}}{\rho_{tol}} \times \left( \frac{m_{wet}}{m_{res}} - 1 \right) \right]$$

$$\%G = \frac{m_{res}}{m_{dry}} \times 100$$

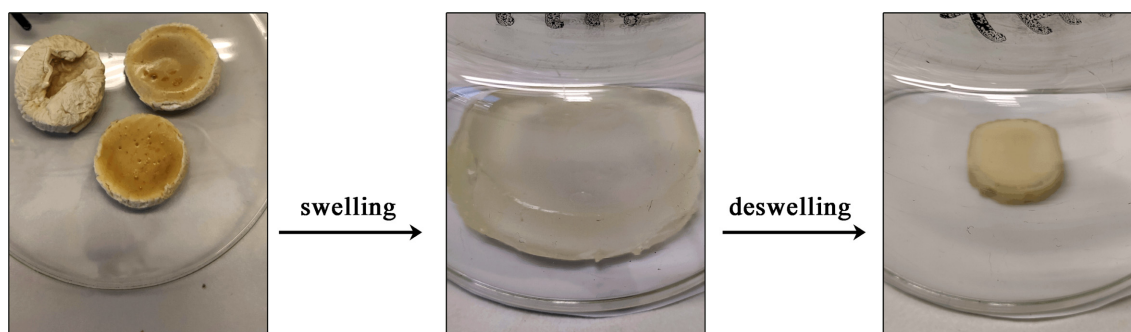


Figure S1. Swelling of the gel (entry 13 of Table 1).

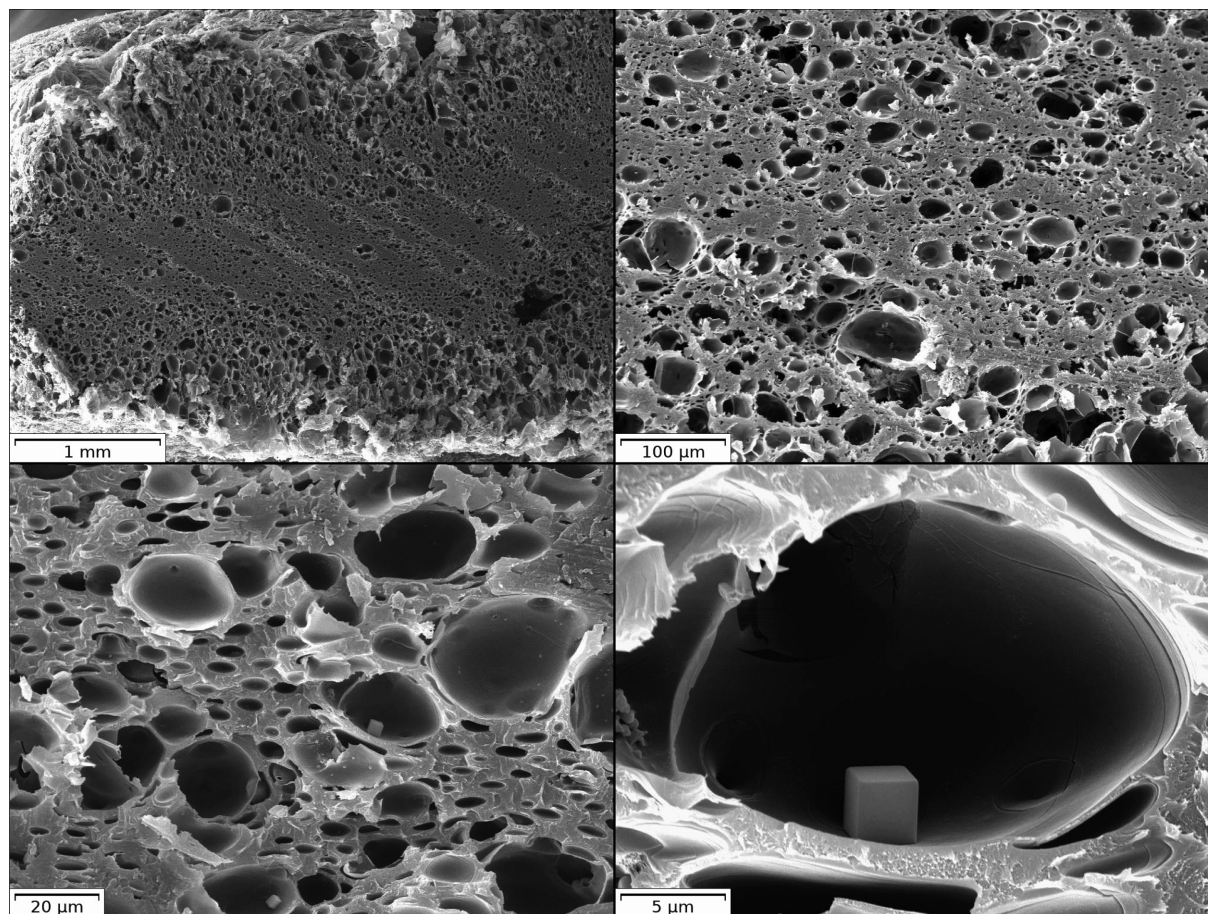
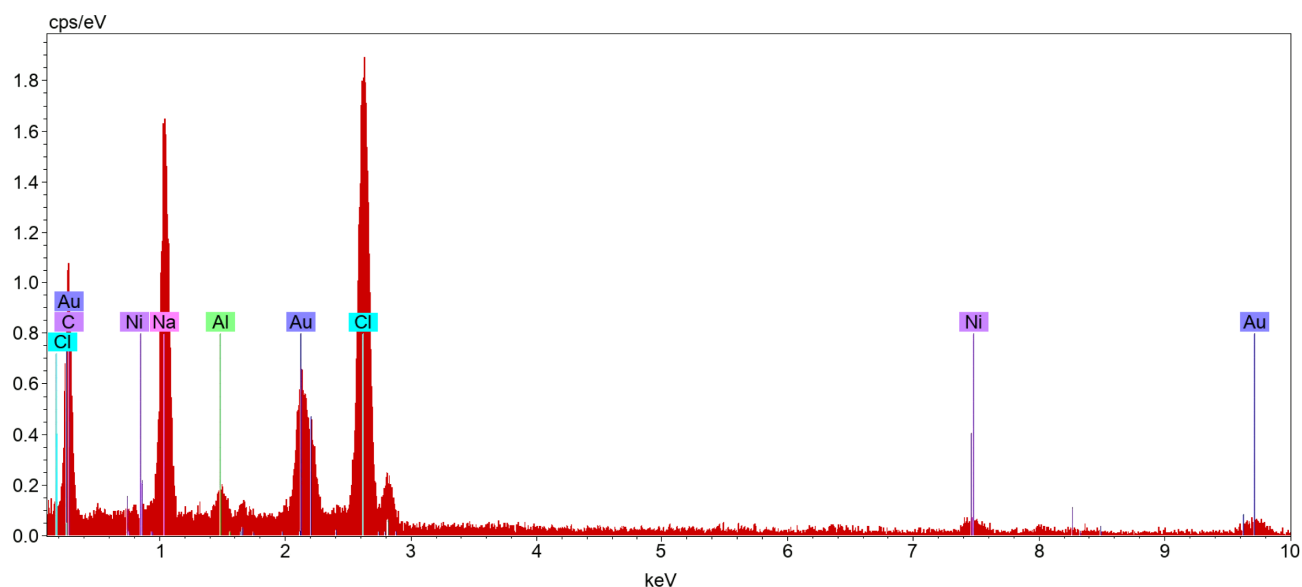
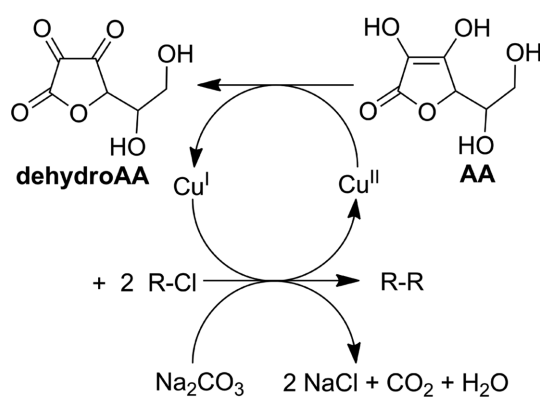


Figure S2. SEM images of a slice of the cross linked PS obtained at 70 °C (entry 13 of Table 1). From top left to bottom right: 70 $\times$ , 500 $\times$ , 2000 $\times$ , and 10 000 $\times$  magnifications.



**Figure S3.** XR spectrum of the cubic crystals inside the cavities of the gel.



**Scheme S1.** The radical coupling (termination reaction) between two chain ends (R·) oxidizes Cu<sup>I</sup> to Cu<sup>II</sup>, which is again reduced by ascorbic acid (AA). Overall, HCl is released and quenched by Na<sub>2</sub>CO<sub>3</sub>.

#### 4. Increment of the initiator concentration

When the [S]<sub>0</sub>:[EDCP]<sub>0</sub> ratio was decreased from 100:1.06 to

100:2.12, after 4.5 h, the reaction mixture showed unexpectedly more fluid (entries 1-2 of Table S2). Moreover, the recovered PS presented low dispersities ( $\mathcal{D} < 1.4$ ) and monomodal GPC curves (Figure 3). Even extending the reaction time to 18 h, only a modest decline of  $\mathcal{D}$  occurred (entry 3 of Table S2). Anyway, the missed correspondence between  $M_n^{\text{th}}$  and  $M_n$  means that a large part of the initiator was consumed by reductive radical coupling processes.

Gelation was finally recovered when the loads of AA and Na<sub>2</sub>CO<sub>3</sub> were doubled (entry 4 of Table S2). The more reducing environment decreases the concentration of Cu<sup>II</sup> in the reaction mixture, thus impairing the control over polymerization.

#### 5. Kinetic study

All the experiments were performed using the same laboratory equipment and glassware. In Table S3 are reported the reactions and their results. The GPC traces are depicted in Figure S4.

**Table S2.** Gelation with 2.12 mol% of EDCP.<sup>a</sup>

Entry	AA/Na <sub>2</sub> CO <sub>3</sub> (mol%)	<i>T</i> (°C)	<i>t</i> (h)	Conv.	<i>M<sub>n</sub></i> (kDa)	<i>M<sub>n</sub><sup>th</sup></i> (kDa)	Δ <i>M<sub>n</sub></i> %	$\mathcal{D}$
1	0.5/1.5	60	4.5	31	3.1	1.7	45	1.30
2	0.5/1.5	70	4.5	48	4.1	2.5	39	1.39
3	0.5/1.5	70	18	75	6.8	3.8	44	1.54
4	1.0/3.0	70	18	gel				

<sup>a</sup>Conditions: [S]<sub>0</sub>:[CuCl<sub>2</sub>]<sub>0</sub>:[TPMA]<sub>0</sub> = 100:0.05:0.05, *V<sub>S</sub>* = 3 mL, *V<sub>EtOAc</sub>* = 3 mL, *V<sub>BzOH</sub>* = 1 mL.

**Table S3.** Kinetics of styrene (S) gelation at 70 °C.<sup>a</sup>

Entry	<i>t</i> (h)	Conv. (%)	<i>M<sub>n</sub></i> (kDa)	<i>M<sub>n</sub><sup>th</sup></i> (kDa)	Δ <i>M<sub>n</sub></i> %	$\mathcal{D}$
1	1.0	16	3.5	1.6	54	1.35
2	2.0	32	10.0	3.3	67	2.00
3	3.25	41	18.3	4.2	77	2.90
4	4.5	46	24.1	4.7	80	3.62
5	6.5	53	32.2	5.4	83	7.47

<sup>a</sup>Conditions: [S]<sub>0</sub>:[EDCP]<sub>0</sub>:[CuCl<sub>2</sub>]<sub>0</sub>:[TPMA]<sub>0</sub>:[AA]<sub>0</sub>:[Na<sub>2</sub>CO<sub>3</sub>]<sub>0</sub> = [100]:[1.06]:[0.05]:[0.05]:[0.5]:[1.5], *V<sub>S</sub>* = 3 mL, *V<sub>EtOAc</sub>* = 3 mL, *V<sub>BzOH</sub>* = 1 mL, *T* = 70 °C.

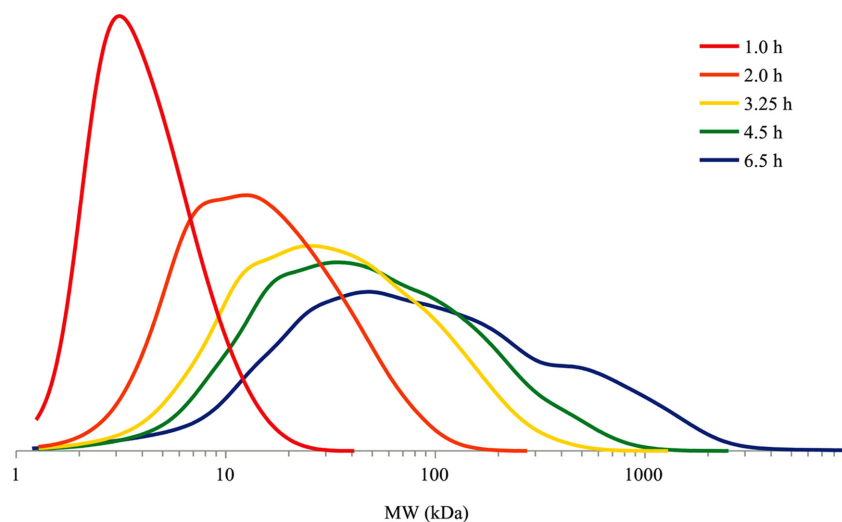


Figure S4. GPC analysis of the kinetic study.

### 6. <sup>1</sup>H-NMR of PS from the kinetic study

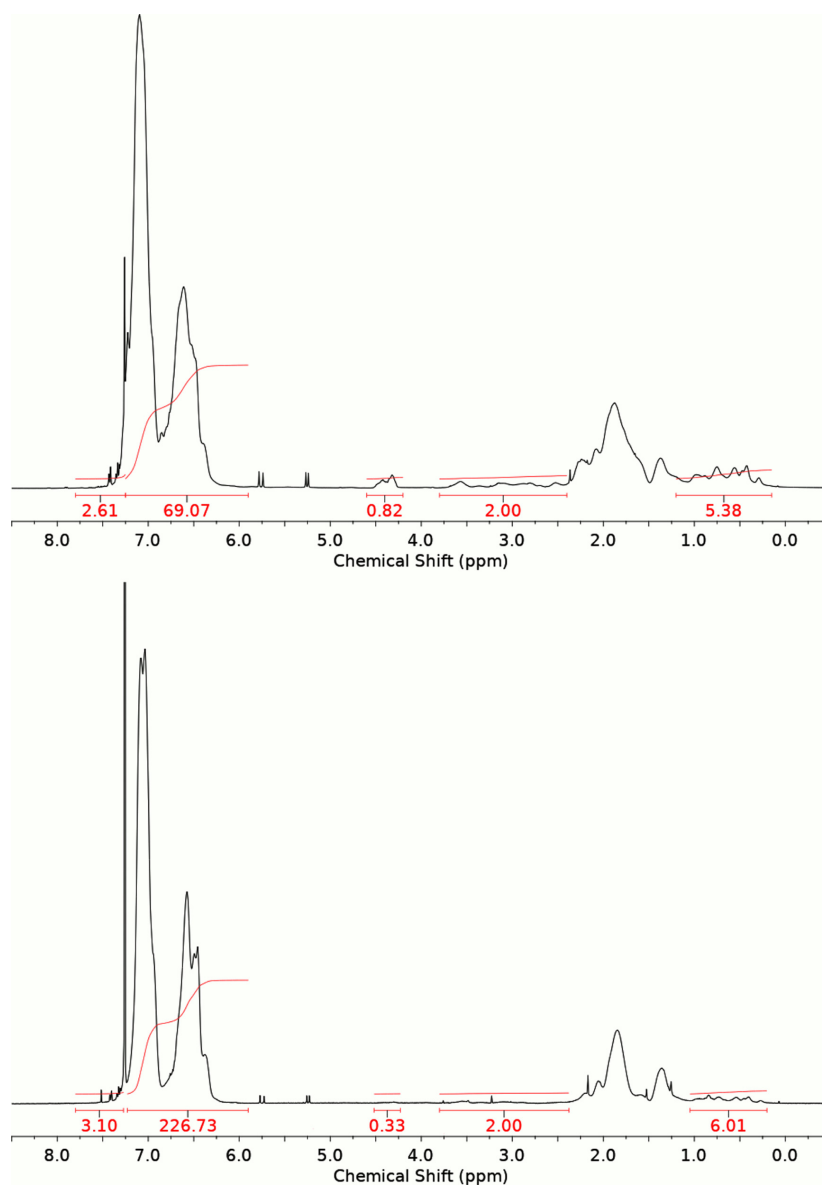


Figure S5. Presaturated <sup>1</sup>H NMR spectra of PS isolated after 1 h (*top*, entry 1 of Table S3) and 6.5 h (*bottom*, entry 5 of Table S3).

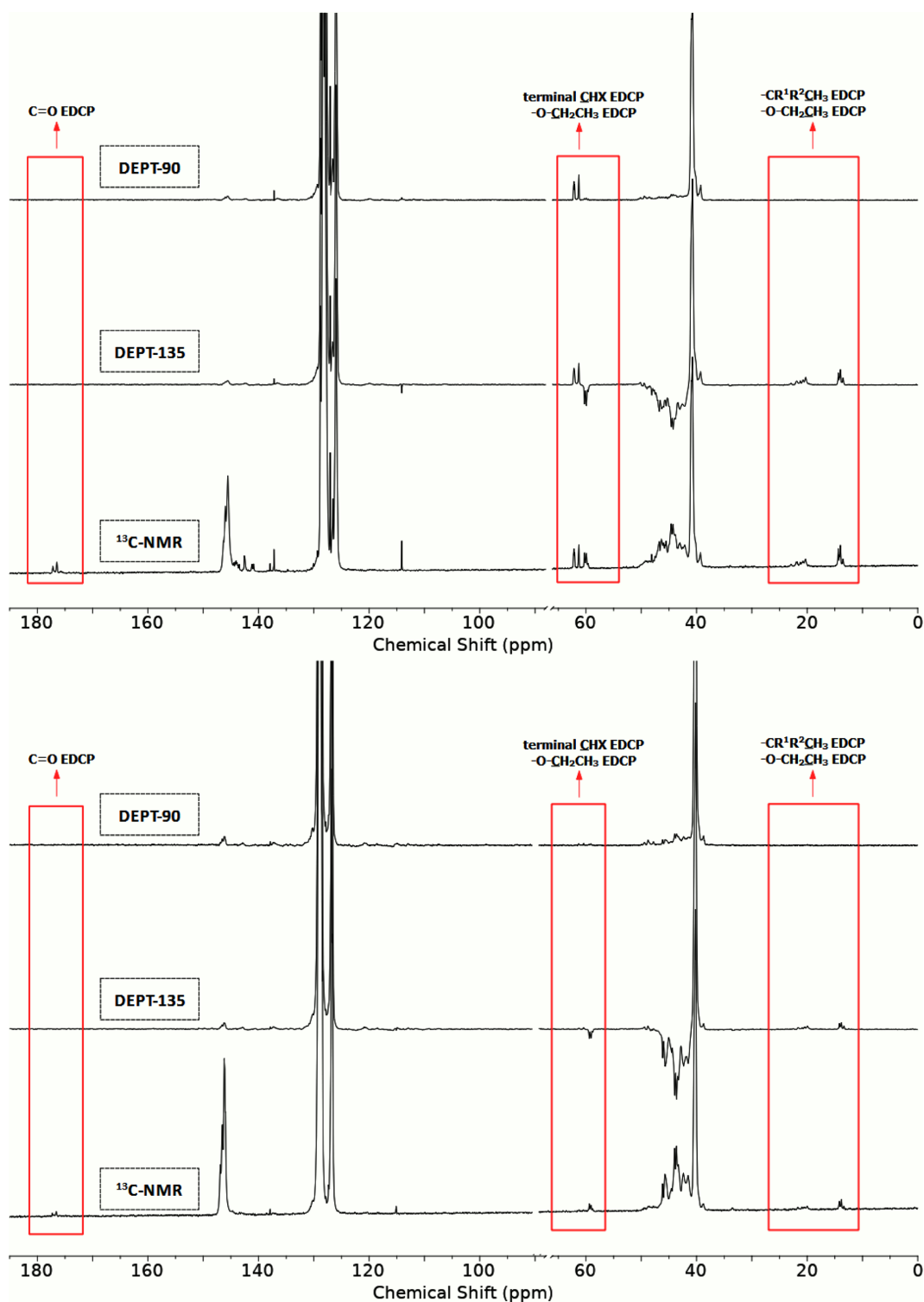


Figure S6. Presaturated  $^{13}\text{C}$  NMR spectra of PS isolated after 1 h (top, entry 1 of Table S3) and 6.5 h (bottom, entry 5 of Table S3).

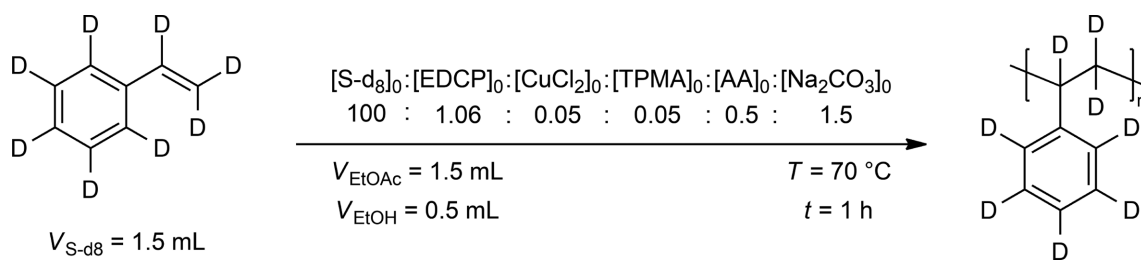
## 7. Polymerization in presence of methyl 2-chloroacrylate (MCA)

Table S4. Polymerization in presence of MCA.<sup>a</sup>

Entry	MCA (mol%)	Conv. (%)	$M_n$ (kDa)	$M_n^{\text{th}}$ (kDa)	$\bar{D}$
1		48	6.5	4.9	1.33
2	0.265	43	6.0		1.34
3	0.53	44	5.5		1.36

<sup>a</sup>Conditions:  $[\text{S}]_0:[\text{EDCP}]_0:[\text{CuCl}_2]_0:[\text{TPMA}]_0:[\text{Na}_2\text{CO}_3]_0 = [100]:[1.06]:[0.2]:[0.2]:[1.5]$ ,  $V_s = 3 \text{ mL}$ ,  $V_{\text{EtOAc}} = 3 \text{ mL}$ ,  $V_{\text{EtOH}} = 1 \text{ mL}$ ,  $T = 70 \text{ }^\circ\text{C}$ ,  $t = 18 \text{ h}$ .

### 8. Synthesis and <sup>1</sup>H-NMR spectrum of deuterated PS



Scheme S2. Synthesis of deuterated PS.

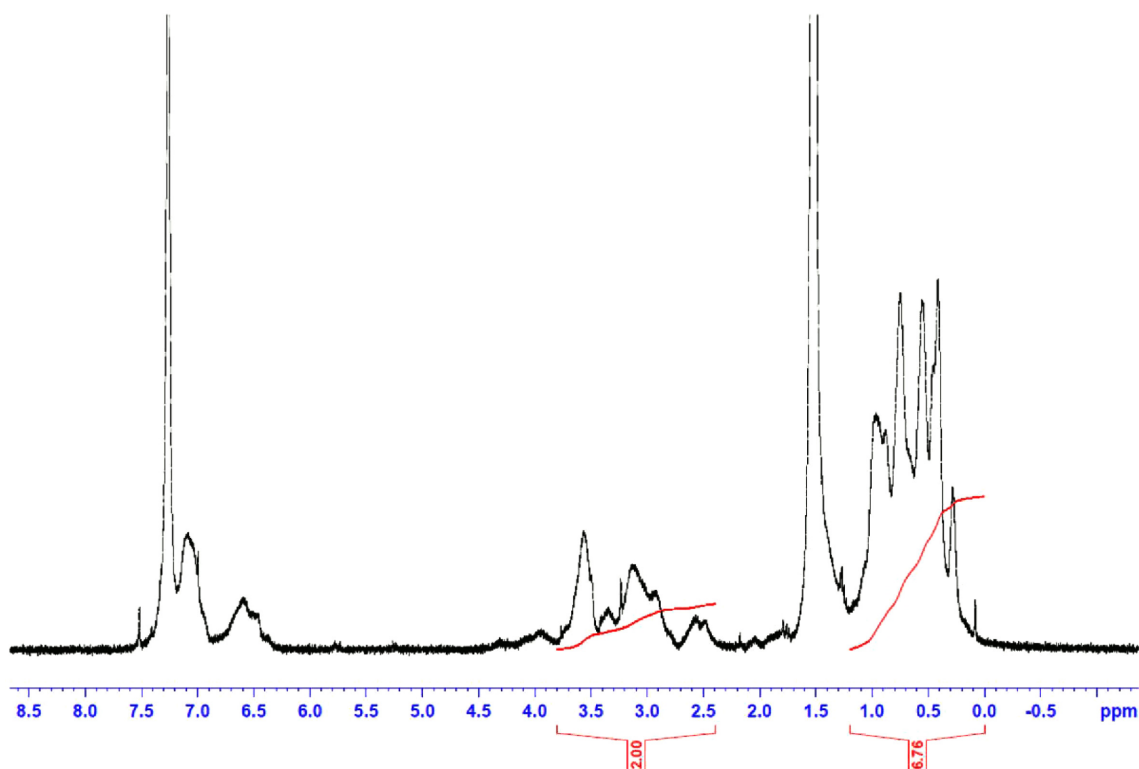


Figure S7. <sup>1</sup>H NMR of the deuterated PS.

### 9. Selected GPC eluograms

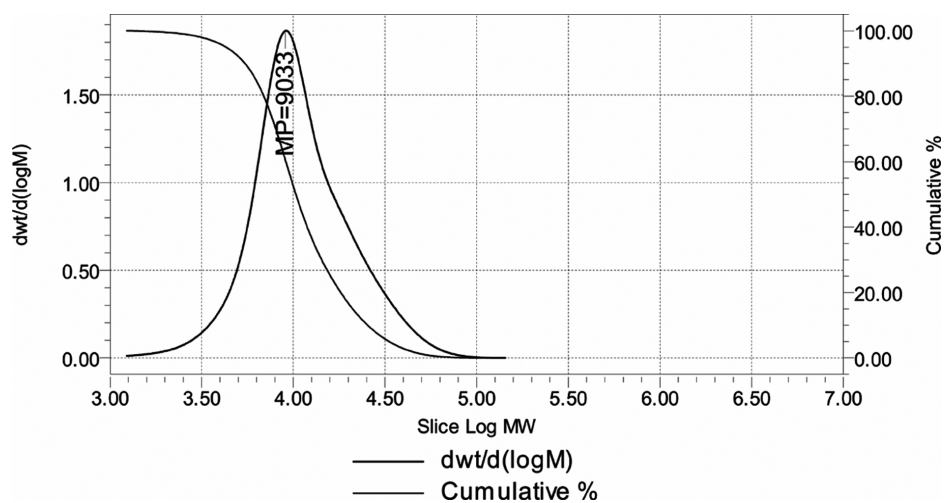
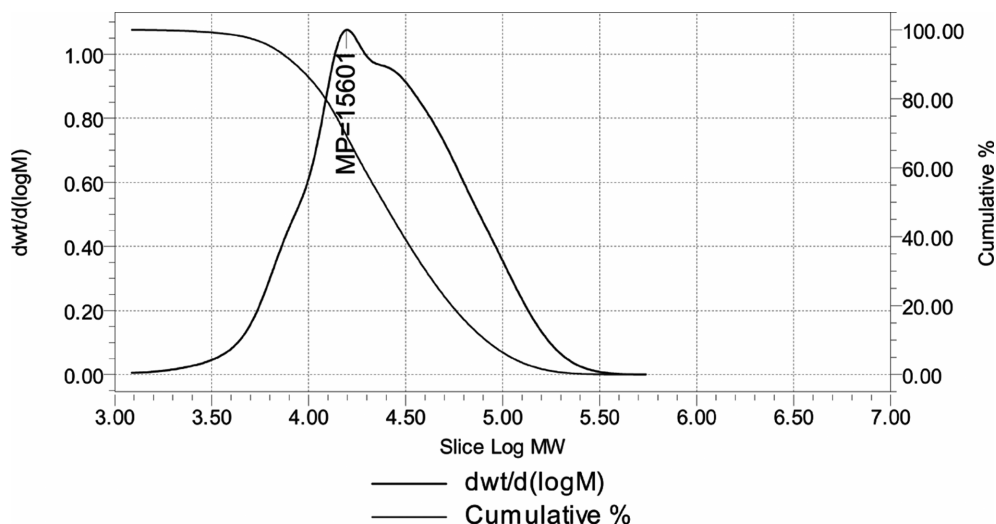
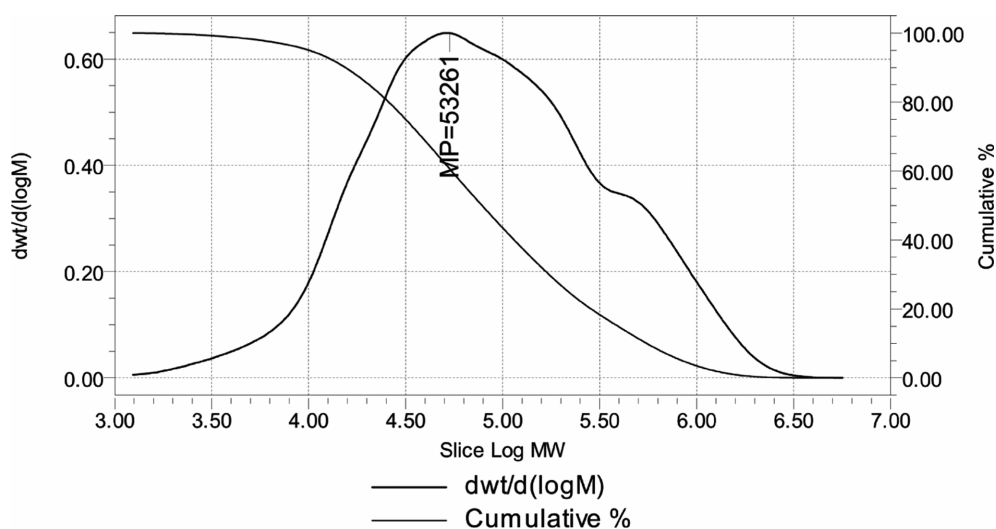


Figure S8. GPC of PS obtained from entry 7 of Table 1. Conditions:  $[S]_0 : [EDCP]_0 : [CuCl_2]_0 : [TPMA]_0 : [AA]_0 : [Na_2CO_3]_0 = 100 : 1.06 : 0.05 : 0.05 : 0.25 : 0.75$ ,  $V_S = 3 \text{ mL}$ ,  $V_{EtOAc} = 3 \text{ mL}$ ,  $V_{EtOH} = 1 \text{ mL}$ ,  $T = 60 \text{ }^\circ\text{C}$ ,  $t = 18 \text{ h}$ .



**Figure S9.** GPC of PS obtained from entry 10 of Table 1. Conditions:  $[S]_0:[EDCP]_0:[CuCl_2]_0:[TPMA]_0:[AA]_0:[Na_2CO_3]_0 = 100:1.06:0.05:0.05:0.5:1.5$ ,  $V_S = 3$  mL,  $V_{EtOAc} = 3.5$  mL,  $V_{EtOH} = 0.5$  mL,  $T = 60$  °C,  $t = 18$  h.



**Figure S10.** GPC of PS obtained from entry 11 of Table 1. Conditions:  $[S]_0:[EDCP]_0:[CuCl_2]_0:[TPMA]_0:[AA]_0:[Na_2CO_3]_0 = 100:1.06:0.05:0.05:0.5:1.5$ ,  $V_S = 3$  mL,  $V_{EtOAc} = 6$  mL,  $V_{EtOH} = 2$  mL,  $T = 60$  °C,  $t = 18$  h.

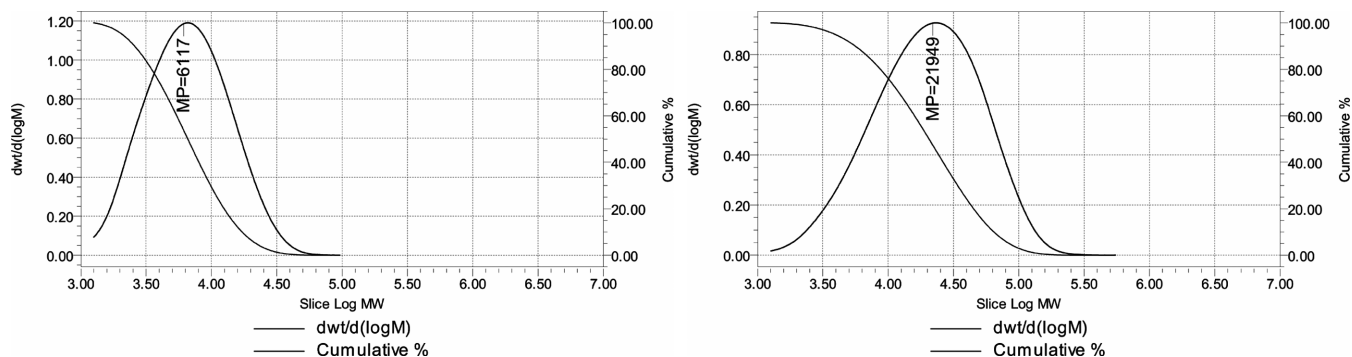


**Figure S11.** GPCs of PSs obtained with tin(II) 2 ethylhexanoate ( $Sn(EH)_2$ ) as reducing agent after 4.5 h (left, entry 4 of Table 2) and 18 h (right, entry 6 of Table 2). Conditions:  $[S]_0:[EDCP]_0:[CuCl_2]_0:[TPMA]_0:[Sn(EH)_2]_0:[Na_2CO_3]_0 = 100:1.06:0.05:0.05:0.5:1.5$ ,  $V_S = 3$  mL,  $V_{EtOAc} = 3$  mL,  $V_{EtOH} = 1$  mL,  $T = 70$  °C.

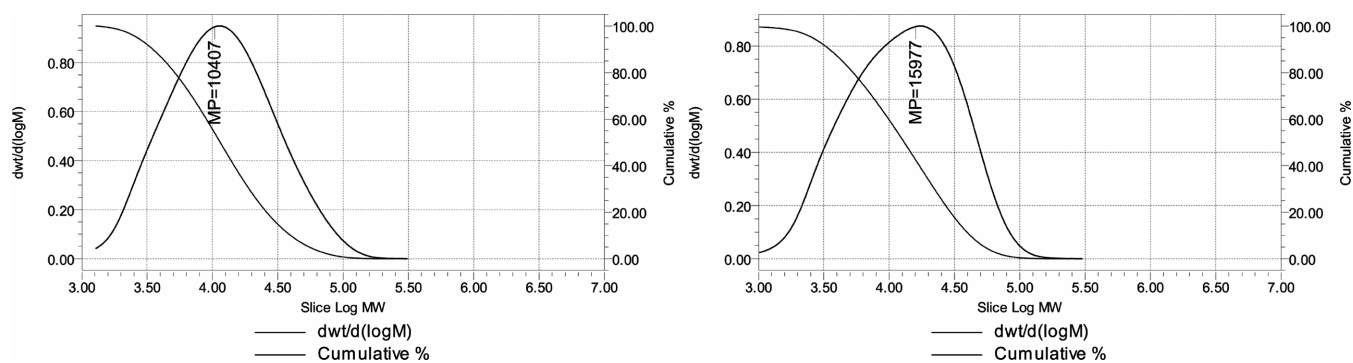


**Figure S12.** GPCs of the PSs obtained with 1.04 mol% (left, entry 8 of Table 2) and 2.08 mol% (right, entry 9 of Table 2) of ECiB. Conditions:  $[S]_0:[CuCl_2]_0:[TPMA]_0:[AA]_0:[Na_2CO_3]_0 = 100:0.05:0.05:0.5:1.5$ ,  $V_S = 3$  mL,  $V_{EtOAc} = 3$  mL,  $V_{EtOH} = 1$  mL,  $T = 70$  °C,  $t = 18$  h.

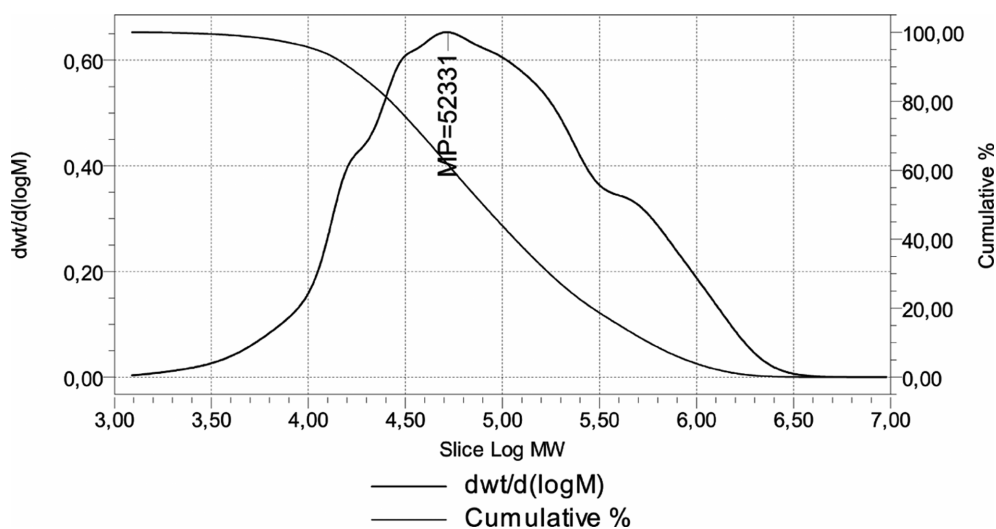


**Figure S13.** GPC of the PS obtained with methyl 2,2 dichlorobutanoate (MDCB) as initiator (entry 10 of Table 2). Conditions:  $[S]_0:[MDCB]_0:[CuCl_2]_0:[TPMA]_0:[AA]_0:[Na_2CO_3]_0 = 100:1.09:0.2:0.2:0.5:1.5$ ,  $V_S = 3$  mL,  $V_{EtOAc} = 3$  mL,  $V_{EtOH} = 1$  mL,  $T = 60$  °C,  $t = 18$  h.

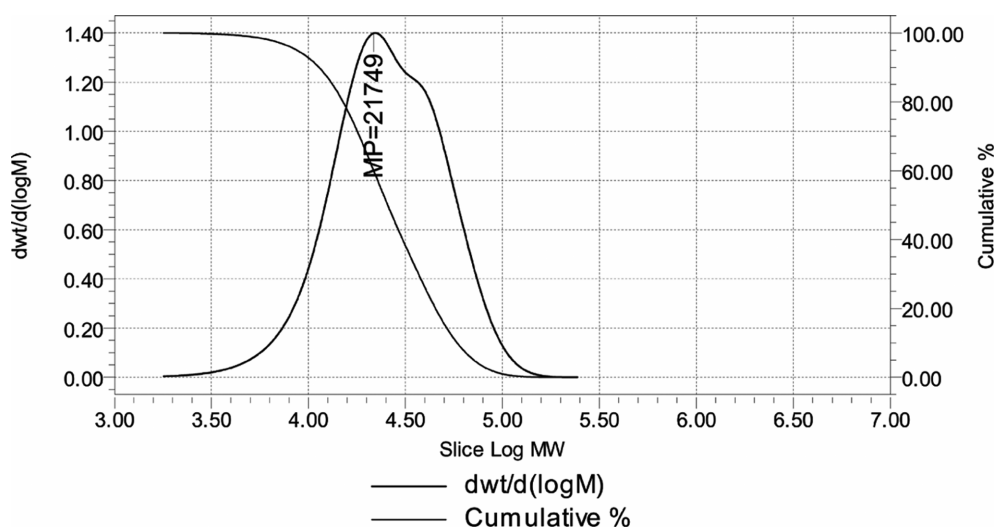


**Figure S14.** GPC of polyethylmethacrylate (PEMA) (entry 13 of Table 2). Conditions:  $[EMA^1]_0:[EDCP]_0:[CuCl_2]_0:[TPMA]_0:[AA]_0:[Na_2CO_3]_0 = 100:1.06:0.2:0.2:0.2:1.5$ ,  $V_S = 3$  mL,  $V_{EtOAc} = 3$  mL,  $V_{EtOH} = 1$  mL,  $T = 60$  °C,  $t = 18$  h.

<sup>1</sup>Ethyl methacrylate

## 10. Dehydrochlorination test on the $\alpha,\omega$ -dichloropolystyrene

A well-controlled  $\alpha,\omega$ -dichloropolystyrene was prepared from EDCP using the “spurious” ARGET ATRP, which employs only  $\text{Na}_2\text{CO}_3$  as reducing agent.<sup>S1</sup> The reaction conditions were  $[\text{S}]_0$ : $[\text{EDCP}]_0$ : $[\text{CuCl}_2]_0$ : $[\text{TPMA}]_0$ : $[\text{Na}_2\text{CO}_3]_0 = [100]:[1.06]:[0.1]:[0.1]:[0.5]$ ,  $V_{\text{S}} = 9 \text{ mL}$ ,  $V_{\text{EtOAc}} = 9 \text{ mL}$ ,  $V_{\text{EtOH}} = 3 \text{ mL}$ ,  $T = 100 \text{ }^\circ\text{C}$ , and  $t = 4.5 \text{ h}$ . The conversion was 47% and the resulting PS had  $M_n = 5030$  and  $D = 1.19$ . The relative GPC chromatogram and the  $^1\text{H}$  NMR spectrum are reported in Figure S15 and Figure S16, respectively.

Entry 4 of Table S3 was repeated replacing EDCP with  $\alpha,\omega$ -dichloropolystyrene (0.26 mmol, 1.30 g) and styrene with toluene (1.5 mL). However, the  $\text{CuCl}_2/\text{TPMA}$  complex was not added.

After 4.5 h at  $70 \text{ }^\circ\text{C}$ , the PS was recovered by precipitation in MeOH as reported in the experimental procedure. The  $^1\text{H}$  NMR spectrum shows that the dehydrochlorination was absent (Figure S17).

The dehydrochlorination test was repeated adding also TPMA (0.013 mmol, 2.8 mg). Even in this case, no elimination was observed (Figure S18).

## References

- (S1) N. Braidì, M. Buffagni, F. Ghelfi, F. Parenti, A. Gennaro, A. A. Isse, E. Bedogni, L. Bonifaci, G. Cavalca, A. Ferrando, A. Longo, I. Morandini, *J. Macromol. Sci. A*, (2021), DOI:10.1080/10601325.2020.1866434.

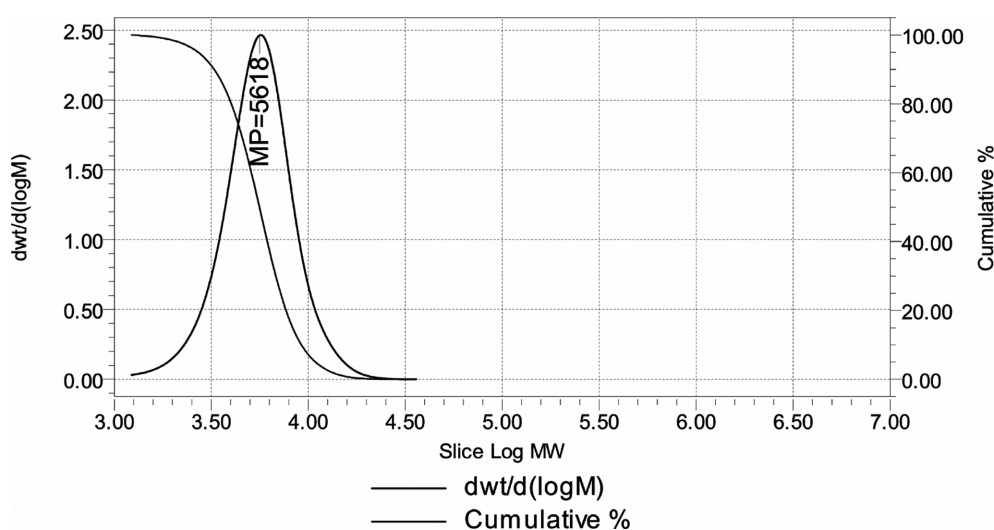


Figure S15. GPC of the  $\alpha,\omega$  dichloropolystyrene used in the dehydrochlorination test.

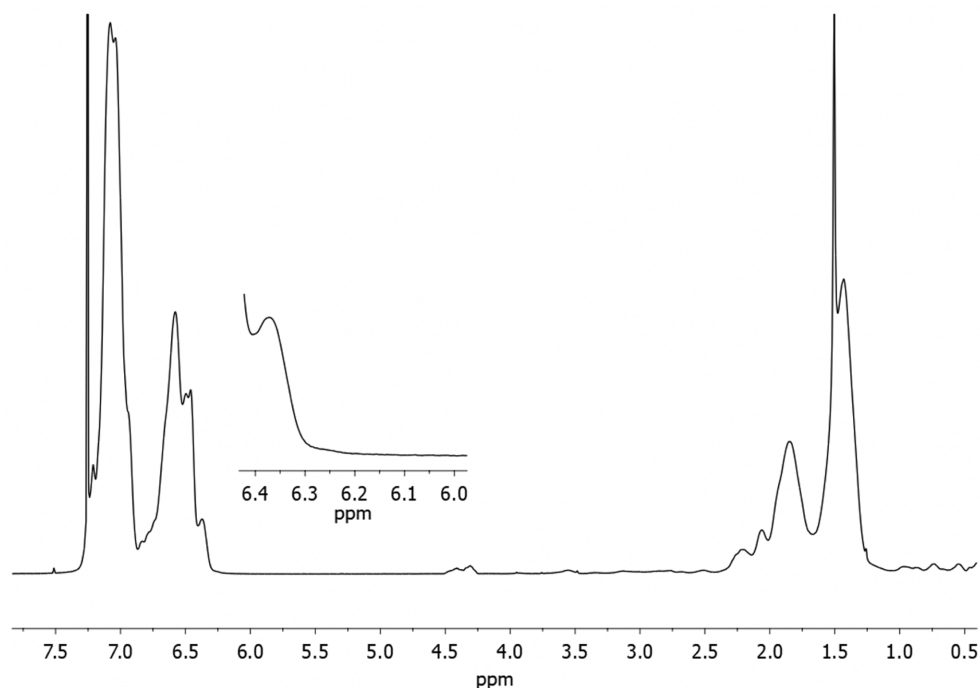


Figure S16.  $^1\text{H}$  NMR of the  $\alpha,\omega$  dichloropolystyrene used in the dehydrochlorination test.

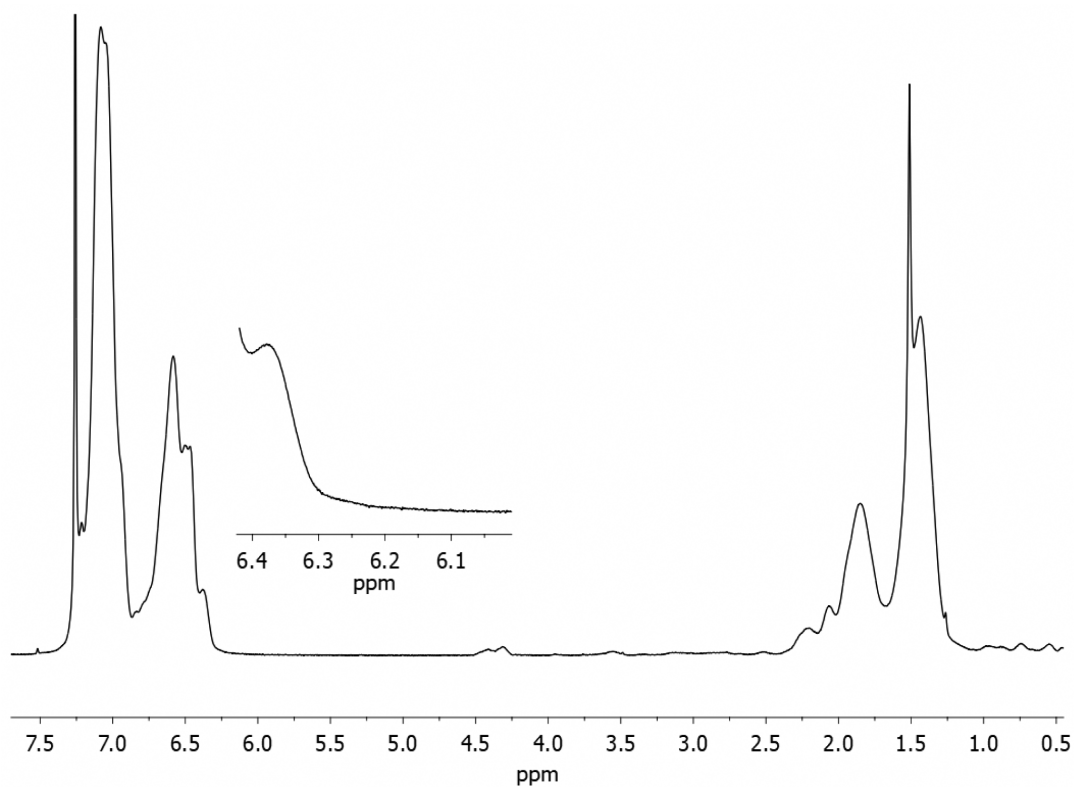


Figure S17. <sup>1</sup>H NMR of the  $\alpha,\omega$  dichloropolystyrene after the dehydrochlorination test.

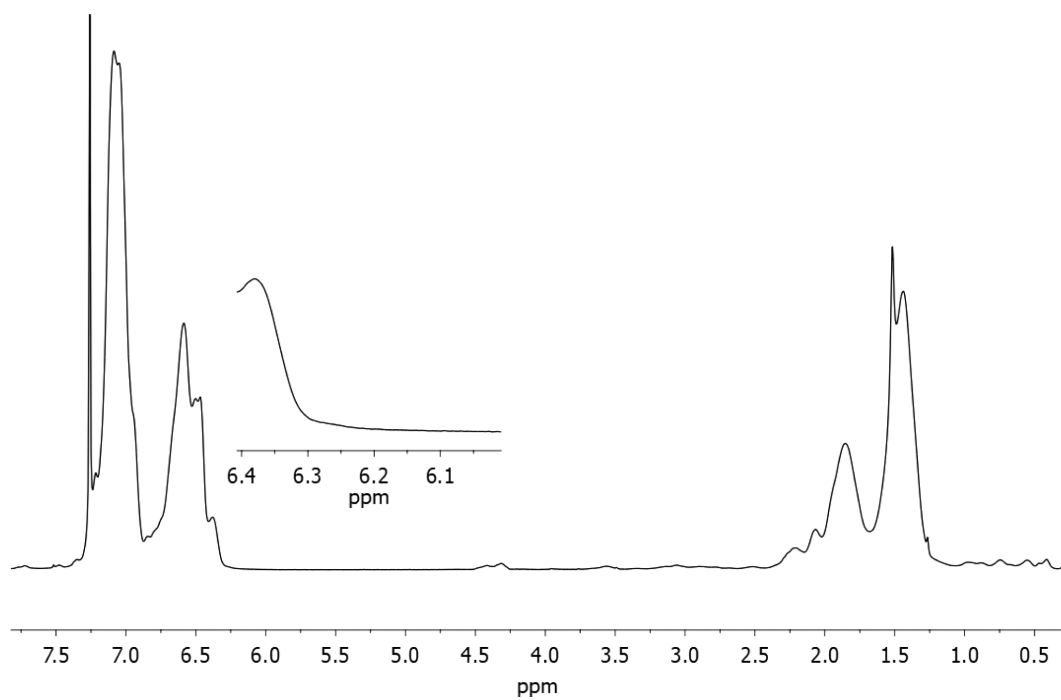


Figure S18. <sup>1</sup>H NMR of the  $\alpha,\omega$  dichloropolystyrene after the dehydrochlorination test in the presence of TPMA.